

Mammals across the K/Pg boundary in northeastern Montana, U.S.A.: dental morphology and body-size patterns reveal extinction selectivity and immigrant-fueled ecospace filling

Author(s): Gregory P. Wilson

Source: *Paleobiology*, 39(3):429-469. 2013.

Published By: The Paleontological Society

DOI: <http://dx.doi.org/10.1666/12041>

URL: <http://www.bioone.org/doi/full/10.1666/12041>

BioOne (www.bioone.org) is a nonprofit, online aggregation of core research in the biological, ecological, and environmental sciences. BioOne provides a sustainable online platform for over 170 journals and books published by nonprofit societies, associations, museums, institutions, and presses.

Your use of this PDF, the BioOne Web site, and all posted and associated content indicates your acceptance of BioOne's Terms of Use, available at www.bioone.org/page/terms_of_use.

Usage of BioOne content is strictly limited to personal, educational, and non-commercial use. Commercial inquiries or rights and permissions requests should be directed to the individual publisher as copyright holder.

Mammals across the K/Pg boundary in northeastern Montana, U.S.A.: dental morphology and body-size patterns reveal extinction selectivity and immigrant-fueled ecospace filling

Gregory P. Wilson

Abstract.—The Cretaceous/Tertiary (K/Pg) mass extinction has long been viewed as a pivotal event in mammalian evolutionary history, in which the extinction of non-avian dinosaurs allowed mammals to rapidly expand from small-bodied, generalized insectivores to a wide array of body sizes and ecological specializations. Many studies have used global- or continental-scale taxonomic databases to analyze this event on coarse temporal scales, but few studies have documented morphological diversity of mammalian paleocommunities on fine spatiotemporal scales in order to examine ecomorphological selectivity and ecospace filling across this critical transition. Focusing on well-sampled and temporally well-constrained mammalian faunas across the K/Pg boundary in northeastern Montana, I quantified dental-shape disparity and morphospace occupancy via landmark- and semilandmark-based geometric morphometrics and mean body size, body-size disparity, and body-size structure via body-mass estimates.

My results reveal several key findings: (1) latest Cretaceous mammals, particularly metatherians and multituberculates, had a greater ecomorphological diversity than is generally appreciated, occupying regions of the morphospace that are interpreted as strict carnivory, plant-dominated omnivory, and herbivory; (2) the decline in dental-shape disparity and body-size disparity across the K/Pg boundary shows a pattern of constructive extinction selectivity against larger-bodied dietary specialists, particularly strict carnivores and taxa with plant-based diets, that suggests the kill mechanism was related to depressed primary productivity rather than a globally instantaneous event; (3) the ecomorphological recovery in the earliest Paleocene was fueled by immigrants, namely three multituberculate families (taeniolabidids, microcosmodontids, eucosmodontids) and to a lesser extent archaic ungulates; and (4) despite immediate increases in the taxonomic richness of eutherians, their much-celebrated post-K/Pg ecomorphological expansion had a slower start than is generally perceived and most likely only began 400,000 to 1 million years after the extinction event.

Gregory P. Wilson. Department of Biology and Burke Museum of Natural History and Culture, 24 Kincaid Hall, University of Washington, Seattle, Washington 98195-1800 U.S.A. E-mail: gpwilson@u.washington.edu

Accepted: 6 March 2013

Published online: 9 May 2013

Supplemental materials deposited at Dryad: doi 10.5061/dryad.gv06d

Introduction

Mass extinctions have had a pronounced effect on the course of evolution (Erwin 1998; Gould 2002; Jablonski 2005; Krug and Jablonski 2012). Beyond the immense losses to biodiversity, these geologically rapid events have deposed successful incumbents, caused the collapse of otherwise stable ecosystems, and, in turn, generated open ecospace and new opportunities for survivors, some of which were previously marginalized but later became dominant. Understanding the dynamics of mass extinctions and their ensuing biotic recoveries thus bears directly on evolutionary and ecological theory, as both aim to explain the loss and origination of biodiversity and

the fragility, collapse, and assembly of ecosystems.

The Cretaceous/Paleogene (K/Pg) mass extinction event offers an ideal opportunity to study mass extinction and biotic recovery dynamics in detail. Although not the most taxonomically severe mass extinction, it was associated with substantial, long-term environmental and biotic effects in both the marine and terrestrial realms (McGhee et al. 2004; Wilson 2005; Krug et al. 2009; Schulte et al. 2010; Archibald 2011; Krug and Jablonski 2012). On land, it signaled the end of Mesozoic dinosaur-dominated faunas and the beginning of an early Paleocene biotic recovery that developed into an unrivaled adaptive radiation of a previously fringe group—eutherian

body size). He emphasized that these correlations hold for modern and background extinctions as well as mass extinctions. In contrast, paleobiologists (Gould 1985; Raup 1986, 1991; Jablonski 1986, 2005) have argued that the rules of selectivity in modern and background extinctions differ from the process in mass extinctions. Mass extinctions with a globally instantaneous, catastrophic kill mechanism, for example, might be nonselective and produce a random pattern of extinction (“field of bullets” scenario of Raup 1991; Archibald 1996; Villier and Korn 2004). In other cases, mass extinctions might exhibit “nonconstructive” selectivity (Raup 1986; “wanton extinction” of Raup 1991; Gould 2002; Jablonski 2005), in which survivorship patterns are neither strictly random nor based on traits that are adaptive (“constructive”) during modern and background times. The most commonly cited example of nonconstructive selectivity is the correlation between survivorship and geographic range above the species level (Jablonski 2005).

Previous studies of the K/Pg mass extinction have inferred or modeled the environmental conditions leading up to and immediately after the K/Pg boundary (see Schulte et al. 2010) and detailed the taxonomic patterns of the extinction among marine and, to a lesser extent, terrestrial ecosystems (see MacLeod and Keller 1996; Wilson 2005, in press; Nichols and Johnson 2008; Archibald 2011). Together, these studies have shed light on the timing, selectivity, rate, magnitude, and causes of the mass extinction (e.g., Marshall and Ward 1996). Coarse ecological assignments of taxa (aquatic vs. terrestrial; infaunal vs. epifaunal) have allowed for some inferences of ecological differences between victims and survivors and discrimination among causal hypotheses (e.g., Sheehan and Fastovsky 1992; Archibald 1996; Sheehan et al. 1996; Markwick 1998; Fara 2000; Vilhena et al. 2012), but few studies have explicitly attempted to quantify ecomorphology across the K/Pg boundary (Lockwood 2004; Wilf et al. 2006; Friedman 2010), particularly for terrestrial vertebrates (Campione and Evans 2011; Wilson et al. 2012; Brusatte et al. 2012), in an effort

to constrain patterns of selectivity and inferred kill mechanisms.

To test for ecomorphological selectivity in the K/Pg extinction of mammals, I compare dental-shape and body-size disparity (sensu Gould 1991; Foote 1993a) of latest Cretaceous mammals and earliest Paleocene local survivors. If the K/Pg extinction was nonselective with respect to dental shape and body size in mammals, then I would predict a random loss of taxa from the dental morphospace and body-size spectrum and, in turn, no changes in disparity across the K/Pg boundary (Foote 1993a). If the mass extinction was selective with respect to either dental shape or body size, then I would predict a nonrandom loss of taxa from the dental morphospace or body-size spectrum, and, in turn, a corresponding change in disparity across the K/Pg boundary. If the regions of the dental morphospace or body size spectrum that experienced the greatest levels of extinction correspond to traits recognized as vulnerable for modern and background extinctions (McKinney 1997: Table 1—specialized diet, large body size), then I would interpret the nonrandom pattern as the product of constructive selectivity. Otherwise, the nonrandom pattern would be interpreted as the product of nonconstructive selectivity.

Biotic Recovery.—Biotic recovery encompasses the re-diversification and ecosystem reconstruction that occur in the aftermath of biodiversity losses and ecological disruption (Droser et al. 1997). Rather than a simple refilling of vacated ecospace through a logistic growth model, recoveries can construct new regions of ecospace (Erwin 2008), exhibit biases (e.g., size bias [Lockwood 2005]), and proceed through a complex dynamic between speciation, immigration, and ecomorphological diversification (Bapst et al. 2012). Biotic recovery from a severe biotic crisis, such as the K/Pg extinction, in which much biodiversity is lost and ecospace emptied, might also transition into evolutionary radiation in which clade expansion is accompanied by increases in taxonomic diversity, ecomorphological diversity, or both. Working hypotheses for the dynamics of recovery and radiation have been synthesized from empirical studies in neo-

TABLE 1. Faunal lists for the latest Cretaceous (Lancian) HCb and earliest Paleocene (Pu1 interval) TUa faunas used in this study. Numbers in parentheses indicate the sample size of lower fourth premolars for multituberculates and lower and upper molars, respectively, for therians.

HCb fauna	TUa fauna
MULTITUBERCULATA	MULTITUBERCULATA
Cimolodontidae	Neoplagiaulacidae
<i>Cimolodon nitidus</i> (10)	<i>Mesodma</i> cf. <i>M. hensleighi</i> (1)
Neoplagiaulacidae	<i>Mesodma</i> cf. <i>M. formosa</i> (26)
<i>Mesodma hensleighi</i> (12)	<i>Mesodma garfieldensis</i> (24)
<i>Mesodma formosa</i> (11)	Taeniolabididae
<i>Mesodma thompsoni</i> (10)	<i>Catopsalis joyneri</i> (4)
? <i>Neoplagiaulax burgessi</i> (6)	<i>Catopsalis alexanderi</i> (1)
Cimolomyidae	Eucosmodontidae
<i>Cimolomys gracilis</i> (4)	<i>Stygimys kuszmauli</i> (26)
<i>Meniscoessus robustus</i> (5)	Microcosmodontidae
<i>Essonodon browni</i> (-)	<i>Acheronodon garbani</i> (1)
<i>Paessonodon nelsoni</i> (1)	" <i>Paracimexomys</i> " group
" <i>Paracimexomys</i> " group	<i>Cimexomys gratus</i> (3)
<i>Cimexomys minor</i> (1)	<i>Cimexomys minor</i> (15)
<i>Paracimexomys priscus</i> (-)	METATHERIA
METATHERIA	Peradectidae
Deltatheridiidae	<i>Thylacodon montanensis</i> (6,5)
<i>Nanocuris improvida</i> (1,1)	EUTHERIA
Stagodontidae	Arctocyoniidae
<i>Didelphodon vorax</i> (9,3)	<i>Protungulatum donnae</i> (15,20)
Pediomyiidae	<i>Protungulatum gorgun</i> (4,4)
<i>Pediomys elegans</i> (6,4)	<i>Baiocodon engdahli</i> (2,1)
? <i>Leptalestes cooki</i> (7,7)	<i>Baiocodon nordicum</i> (5,1)
<i>Leptalestes krejci</i> (7,4)	<i>Oxyprimus erikseni</i> (4,6)
<i>Protolambda hatcheri</i> (8,6)	Periptychidae
<i>Protolambda florenceae</i> (5,4)	<i>Mimatuta minuial</i> (2,3)
Alphadontidae	<i>Mimatuta morgoth</i> (4,3)
<i>Protalphadon foxi</i> (2,5)	<i>Mimatuta</i> sp. indet. (7,-)
<i>Turgidodon rhaister</i> (3,1)	Mioclaenidae
<i>Alphadon marshi</i> (8,5)	<i>Mioclaenid</i> sp. B (1,-)
Herpetotheriidae	Cimolestidae
<i>Nortedelphys jasoni</i> (10,6)	<i>Cimolestes</i> sp. A (1,-)
Glasbiidae	<i>Procerberus formicarum</i> (11,6)
<i>Glasbius twitchelli</i> (11,6)	Palaeoryctidae
EUTHERIA	Palaeoryctid sp. A (2,-)
Gypsonictopidae	Leptictidae
<i>Gypsonictops hypoconus</i> (2,3)	Leptictid sp. A (1,-)
<i>Gypsonictops illuminatus</i> (8,2)	Leptictid sp. B (2,-)
Cimolestidae	
<i>Cimolestes stirtoni</i> (4,3)	
<i>Cimolestes magnus</i> (2,1)	
<i>Cimolestes cerberoides</i> (2,-)	
<i>Cimolestes propalaeorcytes</i> (1,-)	
<i>Cimolestes incisus</i> (3,1)	
Palaeoryctidae	
<i>Batodon tenuis</i> (5,2)	

ecology and paleontology, though the latter is focused mostly on the marine biota, and from equilibrium-based theoretical models (Erwin 2001; Solé et al. 2002). The applicability of these models to terrestrial ecosystems following mass extinction has yet to be fully evaluated, but they provide a basis for structuring hypotheses.

Study of the post-K/Pg biotic recovery has received less attention than the extinction,

despite its importance for understanding the long-term evolutionary consequences of the K/Pg event (Erwin 1998), most notably its presumed role as a watershed event in mammalian evolutionary history. It has long been accepted that when non-avian dinosaurs became extinct at or near the K/Pg boundary, the selective pressures they imposed on mammals (e.g., competition, predation) were relaxed and mammals, particularly eutheri-

ans, rapidly invaded a wide array of “empty” ecological niches (body sizes, diets) via in situ evolution and immigration (e.g., Simpson 1937; Van Valen and Sloan 1977; Archibald 1983, 2011; Stucky 1990; Collinson and Hooker 1991; Alroy 1999). The extinction of large herbivorous dinosaurs may also have indirectly affected mammalian evolution by triggering changes in vegetation structure from relatively open to more closed (Wing and Tiffney 1987; Stucky 1990).

The related view that before the K/Pg boundary mammals were in the “dark ages” has been revised in recent years with discoveries of Jurassic and Cretaceous mammalian skeletons with highly specialized adaptations (see review by Luo 2007) and quantitative analyses that have revealed unexpected ecomorphological diversity in some mostly Mesozoic clades (Wilson et al. 2012). Recent molecular clock studies have also questioned the importance of the K/Pg event in diversification of modern mammalian lineages (e.g., Bininda-Emonds et al. 2007) or pointed to equally significant bursts of diversification that occurred well before the K/Pg boundary (Meredith et al. 2011; see review by Goswami 2012), although statistical analyses of preservation potential in the fossil record deem this early diversification unlikely (Foote et al. 1999). Still, it appears that the first few million years of the Paleocene, which are best documented in the fossil record from the Western Interior of North America, show significant upsurges in mammalian richness, mean body size, and body-size disparity in the aftermath of the end-Cretaceous mass extinction (Stucky 1990; Maas and Krause 1994; Alroy 1999; Smith et al. 2010; Wilson in press). “Within-community” (alpha) richness of eutherians also increased more than fivefold from latest Cretaceous faunas with no more than eight species to early middle Paleocene faunas with greater than 40 species (Cifelli et al. 2004; Lofgren et al. 2004). Although some argue that these increases were driven mostly by archaic lineages (Bininda-Emonds et al. 2007), a post-K/Pg uptick in the rate of chromosomal evolution of modern placental orders (Murphy et al. 2005) further attests to the status of the K/Pg mass extinction event as a mean-

ingful shift in mammalian evolution with substantial long-term implications (Alroy 1999; Archibald 2011).

The rapid post-K/Pg increases in mammalian richness and body size might in turn imply an ecological expansion of mammals with an associated rapid and substantial increase in morphological disparity. Indeed, other clades studied for biotic recoveries and evolutionary radiations (e.g., Cambrian marine arthropods [Foote and Gould 1992]) show that disparity increased more rapidly than did taxonomic diversity, and later stabilized or declined. Counter examples, however, have shown that morphological diversity sometimes increased either after taxonomic diversity increased (e.g., Early Triassic ammonoids [McGowan 2004]) or in step with increases in taxonomic diversity (e.g., Cenozoic mammalian carnivores [Wesley-Hunt 2005]).

Whereas the narrow temporal scope of this study (immediately before and after the K/Pg boundary) precludes an analysis of long-term trends of the post-K/Pg biotic recovery and radiation of mammals, it provides a high-resolution view of the survival phase of the post-K/Pg recovery. By comparing patterns of dental-shape and body-size disparity with taxonomic richness of mammalian paleocommunities I evaluate different aspects of the post-K/Pg recovery, addressing critical questions, such as, Did morphological disparity rebound with taxonomic richness? How was disparity partitioned among taxonomic components of the earliest Paleocene fauna (e.g., immigrants vs. local survivors)? Which aspects of the dental morphospace and body-size spectrum were immediately filled? For example, did archaic ungulates immediately fill the ecomorphological void left by the extinctions of metatherians?

Study Context.—The fossil record of western North America provides the best opportunity for analyzing patterns of mammalian diversity (taxonomic or morphological) across the Late Cretaceous and early Paleocene (Clemens 2001). In this region, the Lancian and Puercan North American Land Mammal “Ages” (NALMAs) span the latest Cretaceous and earliest Paleocene, and the boundary between these NALMAs approximates the K/Pg

boundary. (However, see Cifelli et al. 2004 for a summary of the debate regarding two problematic Canadian assemblages that yield Puercan taxa but are possibly latest Cretaceous in age.) Lancian and Puercan vertebrate fossil assemblages are known from western Canada to Texas (see Cifelli et al. 2004 and Lofgren et al. 2004 for summaries).

Most analyses of mammalian diversity that sample the Lancian and Puercan have binned data at the regional or continental scale (e.g., Maas and Krause 1994; Alroy 1999). Although this approach broadens the spatial coverage and lessens the influence of local oddities, it also agglomerates diversity changes that result from evolutionary and ecological processes operating at multiple spatial scales (e.g., Bambach 1977; Alroy 2000; Badgley 2003). For example, an increase in richness at the regional scale might result from an increase in niche partitioning at the community scale (alpha diversity), an increase in "between-habitat" differences at the regional scale (beta diversity), or some combination of the two.

Other studies have focused at the scale of local fossil assemblages specifically to investigate community-level processes, but because a single study area rarely has multiple well-sampled fossil assemblages from the Lancian and Puercan, the temporal successions, by necessity, have usually been compiled from multiple study areas that are geographically distant from each other (e.g., Archibald 1983; Stucky 1990; but see Maas et al. 1995 and Wilson in press). In such cases, changes through time may reflect not only evolutionary change but also changes related to geographic and paleoenvironmental differences between study areas (Hunter et al. 1997; Hunter and Archibald 2002). Because the aims of this study are to understand paleocommunity-level patterns and processes, I chose to focus at the scale of local fossil assemblages from a single study area. A paleocommunity denotes species associations on a restricted spatiotemporal scale that presume a level of ecological interaction approximating a modern community or biocenosis (Wing et al. 1992). Although fossil assemblages represent thanatocenoses (death assemblages), they may suitably approximate aspects of biocenoses

under certain taphonomic conditions (Behrensmeyer et al. 1992). For the analyses undertaken here (dental-shape and body-size disparity), a fossil assemblage needs only to reasonably reflect the taxonomic composition of the biocenosis; other aspects (e.g., relative abundances of taxa) are not critical to these analyses.

The study area used here is in Garfield and McCone Counties of northeastern Montana (Fig. 1) (Archibald 1982; Lofgren 1995; Clemens 2002; Wilson 2004, 2005, in press). Fossil assemblages from this study area derive from channel-lag and overbank deposits of the Hell Creek and Tullock Formations, and they sample local faunas from the Lancian, Puercan (Pu1 and Pu2/3 interval zones), and Torrejonian (To1 interval zone) NALMAs. I restricted my analyses to the well-studied and well-sampled Lancian local faunas from the upper part of Hell Creek Formation (collectively termed the HCb fauna, herein) and the Pu1 local faunas from the lowermost part of the Tullock Formation in central Garfield County as well as the very top of the Hell Creek Formation in easternmost Garfield and western McCone counties (the TUa fauna, herein). An aim of future research is to expand the scope of this study to include younger Paleocene local faunas, but, at present, the descriptive paleontology of the vast samples of Pu2/3 mammals from the middle Tullock Formation, although underway, is incomplete (e.g., Weil 1998; Clemens 2004, 2006) and To1 local faunas from the upper Tullock Formation require more intensive sampling (Clemens and Wilson 2009). The faunal names (HCb, TUa) stem from an informal subdivision of the assemblages in the study section (HCa, HCb, TUa, TUb, TUb) that is based on chronostratigraphy (Wilson 2004). Tedford (1970) defined a local fauna as fossil assemblages with similar taxonomic composition and from a locality or localities of limited stratigraphic and geographic extent. The fossil assemblages of the HCb fauna have similar taxonomic compositions, but they sample a stratigraphic interval that represents up to 400 Kyr (see below) and multiple depositional events. The same is the case for the TUa fauna. Thus, I refer to each grouping of fossil assemblages as

a fauna, which implies a limited temporal and geographic scope but less so than in a local fauna.

Materials and Methods

Spatiotemporal Framework

The chronostratigraphic framework for the study area (Fig. 1B) integrates the K/Pg boundary clay layer, radiometric ages, and litho-, bio-, and magnetostratigraphic data from multiple sections (see Swisher et al. 1993; Clemens 2002; Wilson 2005, in press). Few other study areas have Lancian and Puercan vertebrate fossil localities tied into such a framework.

The HCb fauna comprises Lancian fossil assemblages from localities that are up to 15 m below the K/Pg boundary and within the Cretaceous part of magnetostratigraphic unit 29r (Wilson 2004, 2005, in press). In central Garfield County, the K/Pg boundary clay layer occurs immediately below the IrZ-Coal, which is at the base of the Tullock Formation (e.g., Moore et al. in press). Renne et al. (2011) provided a revised radiometric age of 66.22 ± 0.06 for a tuff at the base of the IrZ-Coal (Swisher et al. 1993). In easternmost Garfield and western McCone County, the K/Pg boundary is placed a few meters below the Hell Creek-Tullock formational contact on the basis of presence-absence data of Cretaceous palynotaxa (Hotton 2002). Using an estimated duration of ~ 361 Kyr for the Cretaceous part of magnetostratigraphic unit 29r (Ogg and Smith 2004), the HCb fauna is temporally bracketed between 66.58 Ma and 66.22 Ma (Fig. 1B). Relative abundances of mammalian species vary within this interval but taxonomic composition is stable, except the substantial turnover that occurs at or very near the end of this interval (75% local species extinction across the K/Pg boundary [Wilson 2004, 2005, in press]). In this study, the HCb fauna represents a latest Cretaceous paleocommunity.

The TUa fauna comprises Pu1 fossil assemblages from localities that are bracketed in a ~ 15 -m stratigraphic interval between the K/Pg boundary clay layer just below the Hell Creek-Tullock formational contact and the HFZ-Coal in the Tullock Formation (Archibald

1982; Clemens 2002). A tuff from within the HFZ-Coal has yielded a revised radiometric age of 65.81 ± 0.07 Ma (Swisher et al. 1993; recalibration by Renne et al. 2011). In easternmost Garfield and western McCone counties, localities that sample the TUa fauna are within the top few meters of the Hell Creek Formation and the lowermost 3 m of the Tullock Formation, below the McGuire Creek Z-Coal (MCZ-Coal; Lofgren 1995; Clemens 2002). Palynological criteria support a Paleocene age for these fossil assemblages (Hotton 2002). The TUa fauna is thus constrained to the first ~ 410 Kyr of the Paleocene (66.22–65.81 Ma) and likely less, considering that all included localities within this stratigraphic interval are concentrated within several meters of the K/Pg boundary (Fig. 1B). Because mammalian taxonomic composition is consistent across TUa localities (Archibald 1982; Lofgren 1995; personal observation), the TUa fauna is here taken to represent an earliest Paleocene paleocommunity.

This study system should produce patterns that are broadly representative of at least the northern Western Interior of North America. Although the HCb and TUa faunas include only a subset of all known Lancian and Pu1 taxa, respectively (see Cifelli et al. 2004 and Lofgren et al. 2004), they strongly overlap in taxonomic composition with contemporaneous faunas from the northern Western Interior of North America (Weil 1999; Hunter and Archibald 2002). Greater divergence among at least the Lancian faunas occurs in the relative abundances of taxa (Hunter and Archibald 2002; Donohue et al. 2013). Because contemporaneous faunas from outside this region are still relatively poorly known (Clemens 2001; Wilson et al. 2010), it is uncertain how broadly the results might apply beyond the northern Western Interior of North America.

Taxa

Latest Cretaceous and earliest Paleocene mammalian local faunas from North America as well as other Laurasian landmasses include mostly rodentlike multituberculates, metatherians (the stem-based group that includes marsupials), and eutherians (the stem-based

group that includes placentals). The Lancian HCb fauna comprises 31 species, of which there are 11 multituberculates, 12 metatherians, and eight eutherians. The HCb faunal list in Table 1 is based on the detailed studies of Archibald (1982), Lofgren (1995), and Wilson (2004, 2005, in press) with updates to the systematics of the Alphadontidae (Johanson 1996), Herpetotheriidae (Case et al. 2005), Pediomysidae (Fox 1987, 1989; Davis 2007), and Delatheriidae (Wilson and Riedel 2010). Two Lancian taxa, *Paessonodon nelsoni* and *Nanocuris improvida*, that are known from elsewhere are newly identified from the Hell Creek Formation (personal observation). The early Puercan TUa fauna comprises 23 species, of which there are nine multituberculates, one metatherian, and 13 eutherians. The TUa faunal list in Table 1 is based on the detailed studies of Archibald (1982), Lofgren (1995), Wilson (2004, in press), and Clemens (2006), and five newly recognized species that are briefly described in Supplementary Appendix 1. In the text, I refer to these new taxa by informal designations (e.g., Leptictid sp. A). Williamson et al. (2012) recently published a species-level cladistic analysis of nearly all Cretaceous and Paleogene metatherian species. I follow their study in recognizing *Thylacodon* as a valid genus, *T. montanensis* (= *Peradectes* cf. *P. pusillus* of Archibald 1982) as a new species, and *Nortedelphys jasoni* as the new combination resulting from synonymizing *Nortedelphys intermedius* (Case et al. 2005) and *Alphadon jasoni* (Storer 1991). Their higher-level taxonomic reassignments (i.e., removal of *Nortedelphys* from Herpetotheriidae and assignment of *Thylacodon* to Herpetotheriidae), however, are weakly supported and thus not adopted here.

Local Survivors vs. Immigrants.—To distinguish morphological changes across the K/Pg boundary that are due to extinction from those due to immigration, I categorized members of the TUa fauna as either local survivors of the K/Pg event or earliest Paleocene immigrants to the study area (Weil and Clemens 1998; Clemens 2002, 2010). K/Pg local survivors are TUa lineages that are also represented in the latest Cretaceous HCb fauna either by the same taxon or by a plausible ancestor. K/Pg

local victims are those lineages that are present in the latest Cretaceous HCb fauna but absent from the earliest Paleocene TUa fauna in any form. Earliest Paleocene immigrants are lineages that make their first local appearance in the TUa fauna without a plausible ancestor locally present in older faunas (e.g., HCb fauna).

Inference of ancestor-descendant relationships this far back in geologic time and largely without cladistic analyses is problematic (Archibald 1993; Dayrat 2005). Thus, some debate exists over which taxa are K/Pg local survivors and which are earliest Paleocene immigrants (see Clemens 2010; Williamson et al. 2012; Wilson in press). For example, available stratigraphic, biogeographic, and phylogenetic resolution or lack thereof have led some (Clemens 1966, 2010; Wilson in press) to consider members of the Alphadontidae and Herpetotheriidae as possibly ancestral to the Peradectidae. Others, however (Johanson 1996; Horovitz et al. 2009; Williamson et al. 2012), have suggested that recent cladistic analyses point to a much earlier divergence of Peradectidae that precludes an ancestor-descendant relationship with alphadontids or herpetotheriids. In the former case, an ancestor-descendant relationship of an HCb alphadontid (*Alphadon*, *Protalphadon*) and the TUa peradectid (*Thylacodon montanensis*) would mean that this lineage locally survived the K/Pg extinction event. In the latter case, the peradectid *Thylacodon montanensis* likely evolved elsewhere, survived the K/Pg extinction event, and became an earliest Paleocene immigrant to the study area. In unsettled cases such as this, I have opted to interpret TUa taxa as local survivors rather than immigrants, pending greater phylogenetic resolution. An archaic ungulate (*Protungulatum coombsi*) has recently been recorded in the Lancian-age Spigot Bottle local fauna of nearby Carter County, southeastern Montana (Archibald et al. 2011). Its extremely low relative abundance in that assemblage (one out of nearly 1200 mammalian specimens) argues that archaic ungulates (arctocyonids, periptychids, mioclaenids) were mostly if not entirely earliest Paleocene immigrants to the study area. The taeniolabidids (*Catopsalis*

spp.), the microcosmodontid *Acheronodon garbani*, and the eucosmodontid *Stygimys kuszmauli* are also considered post-K/Pg immigrants to the study area.

Quantifying Morphology

Quantifying morphology with the aim of measuring disparity has been a challenge for biologists and paleontologists alike (Rohlf 1990; Gould 1991; Foote 1997). Studies have traditionally relied upon taxonomic proxies to measure mammalian disparity because numbers of higher taxa, such as orders, are relatively easy to tabulate and they often represent distinct adaptive types or ecologies (Simpson 1952; Van Valen 1971; Lillegraven 1972). However, the amount of morphological diversity represented by a higher taxon varies, even within biological groups, such as mammals, thereby limiting the precision and resolution provided by this proxy. Moreover, direct measurement of morphological differences among taxa has shown that disparity patterns and taxonomic patterns are often discordant (e.g., Foote and Gould 1992; Wagner 1995), revealing independent insights into the processes of evolutionary radiation, ecospace filling, and biotic recovery (Foote 1997) and the roles of ecological and developmental constraints (Ciampaglio 2002, 2004).

I directly quantified morphology in terms of dental shape and body size in HCb and TUa mammalian taxa. Not only is the early mammalian fossil record composed mainly of dentulous jaw fragments and isolated teeth, but also dental morphology is tightly linked to feeding ecology in mammals (e.g., Lucas 2004). Thus, dental-shape disparity and morphospace occupancy of HCb and TUa mammals should reflect the diversity of feeding ecologies within latest Cretaceous and earliest Paleocene faunas. Body size is appropriate for this study as well because it is strongly correlated with many important ecological (e.g., trophic strategy, population size) and physiological variables (e.g., metabolism, locomotion) (see Damuth and MacFadden 1990).

Tooth Positions.—For practical reasons, I restricted my dental-shape analyses to certain tooth positions. Herein, I use standard short-

hand notation for dentition: uppercase letters for upper teeth, lowercase letters for lower teeth, and numbers for tooth loci (e.g., M3 for the third upper molar). For the analyses of therians, I used upper and lower molars, specifically, second molars of eutherians (M2, m2) and third molars of metatherians (M3, m3). These teeth tend to have complex shapes, are heavily involved in food breakdown, and are considered more representative of a taxon's molar morphology than the first and last molar positions (e.g., reduced m4 of *Glasbius twitchelli*). Perhaps for these reasons, previous analyses of eutherian molar shapes and features have focused on second molars (e.g., Kay 1975; Strait 1993; Hunter 1997; Gordon 2003). The third molar of metatherians is considered by some to be homologous with the second molar of eutherians (McKenna 1975; Archer 1978; Lockett 1993). Moreover, because latest Cretaceous and earliest Paleocene therians have seven postcanine teeth—eutherians with four premolars and three molars and metatherians with three premolars and four molars—the eutherian second molar and the metatherian third molar occupy functionally analogous positions relative to the jaw fulcrum or mandibular condyle (Janis 1990; Hunter 1997). To check the effect of these tooth choices, I repeated the analyses using the second molar position for metatherians instead of the third; differences in results were minor (data not shown).

Multituberculates lack clear molar cusp homologies with therians, and thus were analyzed separately. I used the lower fourth premolar (p4) because, in multituberculates, the p4 is amenable to shape analysis and taxonomically informative at the species level (e.g., Novacek and Clemens 1977), but like the molars, it is functionally significant (e.g., slicing-crushing cycle and grinding cycle of mastication in ptilodontoids [Sloan 1979; Krause 1982]), and has previously been used to infer feeding ecology (Wilson et al. 2012).

Although phylogeny can confound a purely functional or ecological interpretation of dental morphology (e.g., Kay 1975; Jernvall et al. 2000), certain structures and parameters (e.g., hypocone, shearing crests, orientation patch count) have been repeatedly but variably

emphasized in unrelated lineages with similar feeding ecologies (e.g., Hunter and Jernvall 1995; Strait 1997; Evans et al. 2007). Indeed, developmental mechanisms, in which small changes in cell-signaling pathways can lead to large phenotypic changes (Jernvall 2000; Salazar-Ciudad and Jernvall 2002; Kangas et al. 2004), enhance the evolvability of mammalian teeth. In turn, selection pressures derived from mechanical demands of food sources can lead to rapid evolutionary changes in tooth shape that can overprint evidence of phylogeny (e.g., Gibbs et al. 2000; Jernvall et al. 2000; Naylor and Adams 2001). Nevertheless, the relationship between tooth shape and feeding ecology is complex. Most notably, species may evolve different molar features to the same functional end (Strait 1993); thus, my interpretations are mindful that taxa in different regions of the dental morphospace may be ecologically convergent.

Additional caveats: (1) Because multituberculates and therians are analyzed separately, morphological disparities of these two groups are not directly comparable—only relative patterns can be evaluated. (2) Aspects of the dentition that are not analyzed in this study provide additional information about ecological specialization or morphological separation between species. For example, the massive, bulbous premolars of the metatherian *Didelphodon vorax* have led to inferences of durophagy (Clemens 1968; Lofgren 1992; Fox and Naylor 2006), an interpretation that might not be obtained from molar morphology alone. (3) Feeding ecology is only one axis upon which mammals partition their ecospace—postcranial fossils, for example, can provide information about locomotion and habitat preference. Unfortunately, it is challenging to place postcranial fossils of Lancian and Puercan mammals into a dentally based taxonomic framework because they are sparse and typically found as fragmentary, isolated elements. Nonetheless, ongoing studies have begun assessment of locomotor diversity among Lancian and Puercan mammalian faunas (Borths and Hunter 2008; Berg 2011).

Specimens.—Specimens for the analyses were obtained from the University of California Museum of Paleontology's (UCMP) col-

lection of the HCB and TUA faunas (>3000 cataloged specimens) as well as from smaller collections housed at the Denver Museum of Nature and Science (DMNH), Natural History Museum of Los Angeles County (LACM), Shenandoah Valley Discovery Museum (SVDM), University of Minnesota Vertebrate Paleontology (UMVP), and University of Washington's Burke Museum (UWBM). Despite the overall number of HCB and TUA specimens in these holdings, some species had a limited number of adequately preserved specimens of the chosen tooth positions (all landmarks must be reliably located). I bolstered samples by adding specimens from other fossil assemblages, if the specimens could be confidently assigned to species known from the HCB or TUA faunas. Local faunas from the lower and middle parts of the Hell Creek Formation in Garfield County, Montana (see Fig. 1B) (Wilson 2004, 2005, in press), local faunas from the type Lance Formation in eastern Wyoming (Clemens 1964, 1966, 1973), and the Trochu local fauna in Alberta (Lillegraven 1969) are all Lancian in age and have taxa in common with the HCB fauna (see Cifelli et al. 2004). The Bug Creek assemblages (Sloan and Van Valen 1965) and some of the McGuire Creek assemblages (Lofgren 1995) are more problematic. They are from channel-fill deposits that are reworked across the K/Pg boundary, so they have been of limited use in stratigraphically controlled studies (Lofgren et al. 1990; Clemens 2002). Only specimens from these assemblages with unambiguous temporal origins were included in the samples. For example, *Mesodma thompsoni* is known from Lancian and Pu1 local faunas, so Bug Creek specimens of *M. thompsoni* could not be unambiguously assigned to either the HCB or TUA samples. *Didelphodon vorax* has otherwise only been documented in Lancian local faunas (Cifelli et al. 2004), so Bug Creek specimens of *D. vorax* were included in the HCB sample. *Cimexomys minor* was the only exception; I included specimens from the Bug Creek Anthills in the TUA sample on the basis of its extreme rarity in the HCB fauna. To assess the effect of the expanded sampling, I compared morphological variation in samples from only the

HCB and TUA faunas vs. samples that included other faunas as well. Differences in intraspecific variation were minor, suggesting that the sampling approach did not distort the morphological disparity within the HCB or TUA faunas.

Isolated m2s and m3s of the metatherian *Turgidodon rhaister* are indistinguishable from one another (Clemens 1966), so specimens of this taxon that were cataloged as “m2 or m3” were treated as m3s in this study. The same approach was taken with M2s and M3s of the poorly known *Nanocuris improvida* (Fox et al. 2007; Wilson and Reidel 2010). Because the only known complete m3 of *N. improvida* (DMNH 55343) has a damaged trigonid, I used trigonid fragments with preserved cusps (see Wilson and Reidel 2010) to inform landmark placement. Lower molars of *Mimatuta* are identifiable to species only when associated with the ultimate lower premolar (Lofgren 1995). Thus, isolated m2s identified as *Mimatuta* sp. indet. were plotted in the morphospace but excluded from the disparity calculations, which rely upon the mean shape of a species.

The HCB faunal sample in Table 1 includes 104 lower-molar specimens from all 20 therian species, 64 upper-molar specimens from 18 of 20 therian species, and 60 p4 specimens from nine of 11 multituberculate species. The p4s of *Paracimexomys priscus* and *Essonodon browni* are unknown. The TUA faunal sample includes 67 lower-molar specimens from all 14 therian species, 49 upper-molar specimens from nine of 14 therian species, and 101 p4 specimens from all nine multituberculate species (Table 1). Sampling is more complete for the lower-molar data set than for the upper-molar data set. Bootstrapping and subsampling methods were used to assess the effect of taxon absences on values of disparity (see *Measuring Dental-Shape and Body-Size Disparity*, below), but generally, if the morphology of the omitted species is not expected to diverge strongly from the morphologies of other taxa in the analyses, the effect on disparity should be minimal (Foote 1993b). The highly derived molars of *Essonodon browni*, for example, imply that absence of its p4 in analyses artificially reduces the disparity of HCB multi-

tuberculates. In contrast, the TUA eutherian species without available upper-molar specimens should be morphologically similar to other species in the TUA sample (e.g., Mioclaenid sp. B similar to other archaic ungulates) or the HCB sample (e.g., Leptictid sp. A similar to *Gypsonictops* spp.); thus, their absence should not strongly affect the upper-molar disparity of the TUA therians. Detailed information for all specimens in the analyses is in Supplementary Table 1.

Imaging.—Images of specimens were taken with a digital camera mounted to a dissecting microscope. Therian molars were oriented in occlusal view so as to balance the projection of the buccal, lingual, mesial, and distal bases of the crown (Fig. 2A,B). Multituberculate p4s were oriented in buccal view so that the entire blade was in the same focal plane (Fig. 2C). To minimize distortion and maximize consistency, the tooth was centered and magnified so that it occupied a similar proportion of the viewing field in each image. Although surface relief data of teeth can strengthen ecomorphological inferences (e.g., Evans et al. 2007; Wilson et al. 2012), high-resolution 3-D imaging was impractical and cost prohibitive at the time of study.

Geometric Morphometrics.—I used two-dimensional geometric morphometrics for dental-shape analysis. In this approach, the configuration of landmarks (LMs) represents the shape of a tooth. I identified LMs that capture functionally important aspects of molar morphology, represent homologous features that are present in all taxa included in the analysis, and can be found repeatably and reliably on all specimens (Zelditch et al. 2004). I also used semilandmarks (SLMs) to capture other significant components of tooth shape (e.g., curvature of the protoconal base) that could not be represented as LMs. Although individual SLMs are comparable rather than homologous points along a curve or shape, the curve or shape as a whole may be homologous. To avoid excessive weighting of one morphological feature in the analyses, some points along the curve were designated as helper points and used only for superimposition. The remaining points, the SLMs, were used in superimposition and geometric

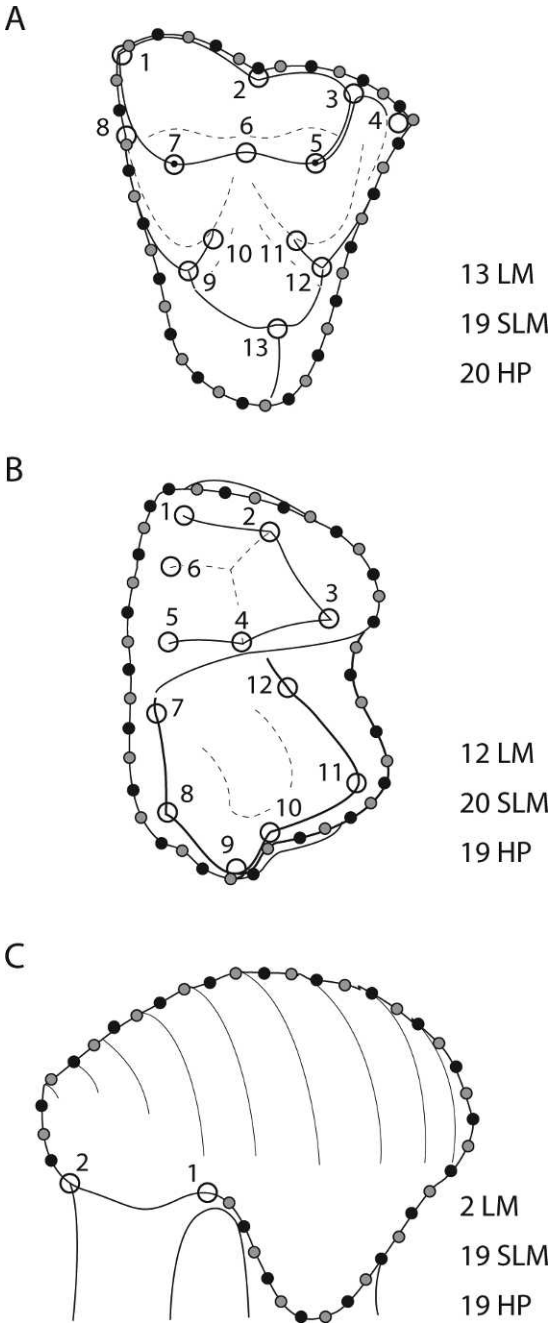


FIGURE 2. Digitization schemes for geometric morphometric analyses of therian upper (A) and lower (B) molars, and for multituberculate lower fourth premolars (C). Landmarks (LM) are shown as large open circles, semi-landmarks (SLM) as small black circles, and helper points (HP) as small grey circles.

morphometric analyses. The LMs, SLMs, and helper points that were used in my analyses are illustrated in Figure 2 and described in Table 2. To measure the effects of using SLMs, I ran a parallel set of analyses on the therian data sets using only LMs; the disparity patterns do not differ and the morphospace plots show only minor differences (see Supplementary Fig. 1).

Using tpsDig version 2.16 (Rohlf 2010a), I digitized LMs on specimen images and converted them into two-dimensional Cartesian coordinates (x, y). For SLMs, the feature of interest (e.g., occlusal outline of the molar) was traced using the pencil tool in tpsDig version 2.16, and the resulting curve was resampled for a specific number of points that were evenly distributed by length. Points along the curve were initially converted to LMs in tpsUtil version 1.46 (Rohlf 2010b). Generalized least-squares (GLS) Procrustes superimposition of the LM configurations was performed with CoordGen6f (Sheets 2003) of the Integrated Morphometrics Package (IMP). GLS Procrustes superimposition removes all differences between LM configurations that are due to scale, rotation, or translation, leaving only differences due to shape (sensu Kendall 1977). After superimposition, I designated SLMs and helper points in Semiland6 for IMP (Sheets 2009). Then, LM and SLM coordinates were converted to partial warp scores, which are shape coefficients that employ Procrustes distance and have the appropriate degrees of freedom for use in subsequent analyses (e.g., principal components analysis).

Estimating Body Size.—I estimated body mass in HCB and TUA mammals by using taxon- and morphology-appropriate predictive formulae from regression analyses of m1 area and body mass in extant mammals (Bloch et al. 1998 for eutherians; Smits and Wilson 2011 for metatherians; Wilson et al. 2012 for multituberculates). Acknowledging that body-mass estimates in extinct mammals have uncertainties (Fortelius 1990; Damuth 1990), these estimates, unlike the dental-shape data, can be compared across all members of the HCB and TUA faunas. The m1s of the HCB multituberculates *?Neoplagiaulax burgessi* and

TABLE 2. Description of landmarks and semilandmarks used in this study. See Figure 2 for corresponding illustrations.

Landmarks and semilandmarks	
THERIAN LOWER MOLARS	
Landmarks	
1, 3, 5, 8, 9, 11	Apices of the main cusps (paraconid, protoconid, metaconid, entoconid, hypoconulid, and hypoconid, respectively)
2, 4	Ventralmost points of the paracristid (i.e., paracristid notch) and protocristid (i.e., protocristid notch), respectively
6	Lingualmost edge of the notch between the paraconid and metaconid
7	Ventralmost point of the entocristid (i.e., talonid notch)
10	Ventralmost point of the posthypoconid; usually convergent with the contact between the cristid that extends mesiobuccally from the hypoconulid and the cristid that extends distolingually from the hypoconid
12	Ventralmost point of the cristid obliqua nearest the contact with the distal aspect of the trigonid
Semilandmarks	
13–32	Full outline of the occlusal view of the crown starting and ending at landmark 1, excluding mesial and distal cingulids
THERIAN UPPER MOLARS	
Landmarks	
1	Point of contact between the postmetacrista and ectocingulum; often manifest as a metastyle or stylar cusp E in metatherians
2	Lingualmost point of the ectoflexus
3	Point of contact between the preparacrista and the ectocingulum; often manifest as a stylocone or stylar cusp B in metatherians
4, 8, 10, 11	Buccal terminations of the cristae of the premetaconule, postmetaconule, premetaconule, and postparaconule, respectively; in specimens that have faint traces of these cristae on the lingual face of the metacone or paracone, the dorsalmost point lingual to that trace was used; buccal termination of the premetaconule crista is often manifest as a parastyle or stylar cusp A in metatherians
5, 7, 13	Apices of the main cusps (paracone, metacone, and protocone, respectively)
6	Apex of the centrocrista
9, 12	Apices of the conules (metaconule and paraconule, respectively)
Semilandmarks	
14–32	Full outline of the occlusal view of the crown starting and ending at landmark 1
MULTITUBERCULATE LOWER FOURTH PREMOLARS	
Landmarks	
1	Dorsalmost point of the ventral edge of the enamel between the two roots
2	Point of contact between the distal aspect of the crown and the distal root
Semilandmarks	
3–21	Partial outline of the lateral profile of the crown counterclockwise from landmark 1 to landmark 2

Paressonodon nelsoni and the TUA *Acheronodon garbani* are unknown, so these taxa were excluded from the body-size analyses. The m1s of TUA eutherians *Cimolestes* sp. A, *Palaeoryctid* sp. A, *Leptictid* sp. A, and *Leptictid* sp. B are also unknown, but because m2s of eutherians are typically only slightly larger than m1s, m2 measurements of these taxa were substituted for these analyses. Tooth area was approximated as the product of length and width dimensions reported in the literature and from direct measurements. Body-mass estimates are in Supplementary Tables 2 and 3.

Measuring Dental-Shape and Body-Size Disparity.—Disparity describes the magnitude of morphological differences among members of a taxonomic group, fauna, or temporal interval. It can be measured many ways (see Foote 1997), each of which has advantages and disadvantages depending on the type of data available and the questions being addressed (see Ciampaglio et al. 2001). I measured disparity as a variance of all species shapes (or sizes) from the grand mean species shape (or size). Variances are relatively insensitive to sample size, they do not suffer from the problems associated with metrics based on

volume (Ciampaglio et al. 2001; Zelditch et al. 2004), and they are additive, which is a property that allows the assessment of an individual taxon's contribution (partial disparity) to the overall disparity of the larger group (Foote 1993b). Using the IMP program DisparityBox6i (Sheets 2007), dental-shape disparity was calculated as a variance (MD_v) according to the formula

$$MD_v = \frac{\sum_j^N d_j^2}{(N - 1)}$$

where d_j is the Procrustes distance of the centroid shape for each species j (mean shape of all specimens for that species) from the overall centroid shape (the grand mean shape for all species in an analysis). N is the number of species in an analysis. This formula is equivalent to that given by Foote (1993b) when there is only one group. Disparity was calculated for ten subdivisions of the latest Cretaceous (HCb) and earliest Paleocene (TUa) faunas: HCb therians, HCb eutherians, HCb metatherians, HCb multituberculates, TUa therians, TUa eutherians, TUa archaic ungulates, TUa multituberculates, TUa therian local survivors, and TUa multituberculate local survivors. In each case, the grand mean shape that was used to calculate d_j was derived from the group of interest only. The 95% confidence intervals and standard errors for disparity were estimated by two bootstrapping routines. In the first routine, specimens within species samples for a group of interest were resampled with replacement (2500 bootstraps) to estimate uncertainty in disparity due to specimen sampling. In the second routine, species means within a group of interest were resampled (2500 bootstraps) as a means of estimating variability in disparity due to species sampling. Partial disparity values (PD_v) were calculated for each taxon in the HCb therian, TUa therian, HCb multituberculate, and TUa multituberculate analyses.

To assess the statistical significance of differences in disparities (e.g., HCb Theria vs. TUa Theria), I tested two null hypotheses: (1) inadequate or variable sampling of specimens within each species could give rise to as large a difference in disparity by chance; and

(2) random assignments of species to one group (e.g., HCb Theria) or the other group (e.g., TUa Theria) from a single pool of species could give rise to as large a difference in disparity by chance. Null hypothesis 1 was not rejected if the 95% confidence intervals produced by the specimen-based bootstrapping routine overlapped, even though this approach might lead to failure to reject a false null hypothesis (Type II error) in some cases. Null hypothesis 2 was tested by using a permutation routine in DisparityBox6i. The residual of the centroid shape of each species from the overall centroid shape for each group (e.g., HCb Theria, TUa Theria) was calculated and randomly reassigned to one of the two groups. The difference in disparities between the two groups was then calculated. The level of significance of the observed difference in disparities (i.e., p -value) was estimated from the distribution of differences in 1000 permutations. Note that the sensitivities of the permutation test and the F -test (below) are highly dependent on degrees of freedom. To yield an F -statistic with a significant p -value (<0.05) in a comparison of disparities of two groups with few species (e.g., HC Theria with 20 species vs. TUa local survivors with six species), the disparity of the first group must be much greater than that of the second group (e.g., 4.6 times greater). In the context of differences in disparity that are commonly reported in the literature as significant (1.5 to 3.0 times greater [Foote 1993a; McGowan 2004; Friedman 2010]), these tests may, in some cases (low degrees of freedom), impose an overly high burden of proof and thus be prone to Type II error.

Body-size disparity was calculated as a variance of the body-mass estimates in each taxonomic grouping of interest (e.g., HCb Mammalia). Confidence intervals and standard errors were estimated by bootstrap analyses (1000 times) in Resampling Stats for Excel version 4.0 (Bruce 2012). Statistical significance of differences in body-size disparities between taxonomic groupings (e.g., HCb Mammalia vs. TUa Mammalia) was assessed by an F -test, whereas statistical significance of differences in mean body sizes was assessed using a t -test. I also performed a logistic

regression to quantify the relationship between body size and K/Pg survivorship (Supplemental Appendix 2). The distribution of body sizes in each fauna was visualized by plotting \ln body mass vs. body-mass rank of each species (Fig. 3F).

Mapping Dental Morphospace Occupancy.—Principal Components Analysis (PCA) was used to visualize the morphospace occupancy of the HCB mammalian fauna during the latest Cretaceous and the later filling of that morphospace by the earliest Paleocene TUA mammalian fauna. Using the IMP program PCAGenMac7a (Sheets 2012), PCA was performed on three data sets (therian lower molars, therian upper molars, multituberculate p4s). For each analysis, the following steps were taken: (1) GLS Procrustes superimposition was performed on the combined HCB and TUA data set; (2) partial warp scores were computed from the superimposition, using the mean shape based on all of the data; (3) PCA was conducted on the variance-covariance matrix of the partial warp scores for the latest Cretaceous HCB data set only; and (4) the partial warp scores of the earliest Paleocene TUA data set were then projected onto the HCB-defined PC axes. Consequently, only the HCB data set influenced the relative ordination of taxa, which is appropriate for exploring questions that are framed with reference to the morphospace that was established by the latest Cretaceous HCB mammalian fauna.

The principal components (PCs) that explain at least 10% of the variance in a data set are considered most biologically meaningful (e.g., Tseng and Wang 2011). Only the first three PCs in each of my analyses explain this amount of variance. Scores on these PCs are visualized in bivariate plots for each analysis (PC1 vs. PC2 in Figs. 4, 5, 7 and PC1 vs. PC3 in Fig. 6, Supplementary Figs. 2, 3). Supplementary Table 6 provides eigenvalues and percent variance explained by PCs in each analysis. I used Anderson's (1958) test in PCAGenMac7a to determine whether the amount of variance explained by successive PCs in an analysis was significantly different.

The relative shape changes at the extreme values of the PCs were inferred from the PC coefficients and the original shape variables

(LMs and SLMs) and are graphically represented in the bivariate plots by thin-plate spline deformation grids and vectors at the positive and negative ends of each axis. The configuration of filled circles on the deformation grids represents the mean tooth shape (score of zero). The deformation grid and vectors stemming from the filled circles represent the relative shape change at the extreme value of each PC.

Results

Dental-Shape Disparity among Therians (Table 3, Fig. 3A,B, Supplementary Tables 4, 5)

The absolute values of dental-shape disparity differ among the therian analyses in part because of the differences in the tooth position used (upper molars vs. lower molars) and the numbers of LMs and SLMs used in each analysis (Ciampaglio et al. 2001). Nevertheless, the overall patterns of dental-shape disparity are largely consistent across analyses.

HCB Therians.—Metatherians make up 60% of therian species in the HCB fauna and contribute nearly 70% to the disparity of HCB therians (Table 3). In the lower-molar analysis, the morphologically distinctive but rare delatheridiid *Nanocuris improvida* contributes more to the disparity of HCB therians (31.5%) than any other species. The metatherian *Glasbius twitchelli* (10.4%) and the eutherian *Cimolestes propalaeoryctes* (7.8%) also have high partial disparities. The pediomyid and cimolestid families, each of which has five species in the HCB fauna, contribute 15.1% and 21.0%, respectively, and alphadontids (three species) and gypsonictopids (two species) contribute 5.4% and 6.6%, respectively, to the lower-molar shape disparity of HCB therians.

Partial disparities are more evenly distributed across species in the upper-molar analysis (Table 3). *Nanocuris improvida* again has the highest partial disparity of any species (13.9%), followed by the eutherian *Gypsonictops illuminatus* (9.8%). The Pediomyidae contributes 22.5% and the Alphadontidae, Gypsonictopidae, and Cimolestidae each contribute over 10% to the upper-molar shape

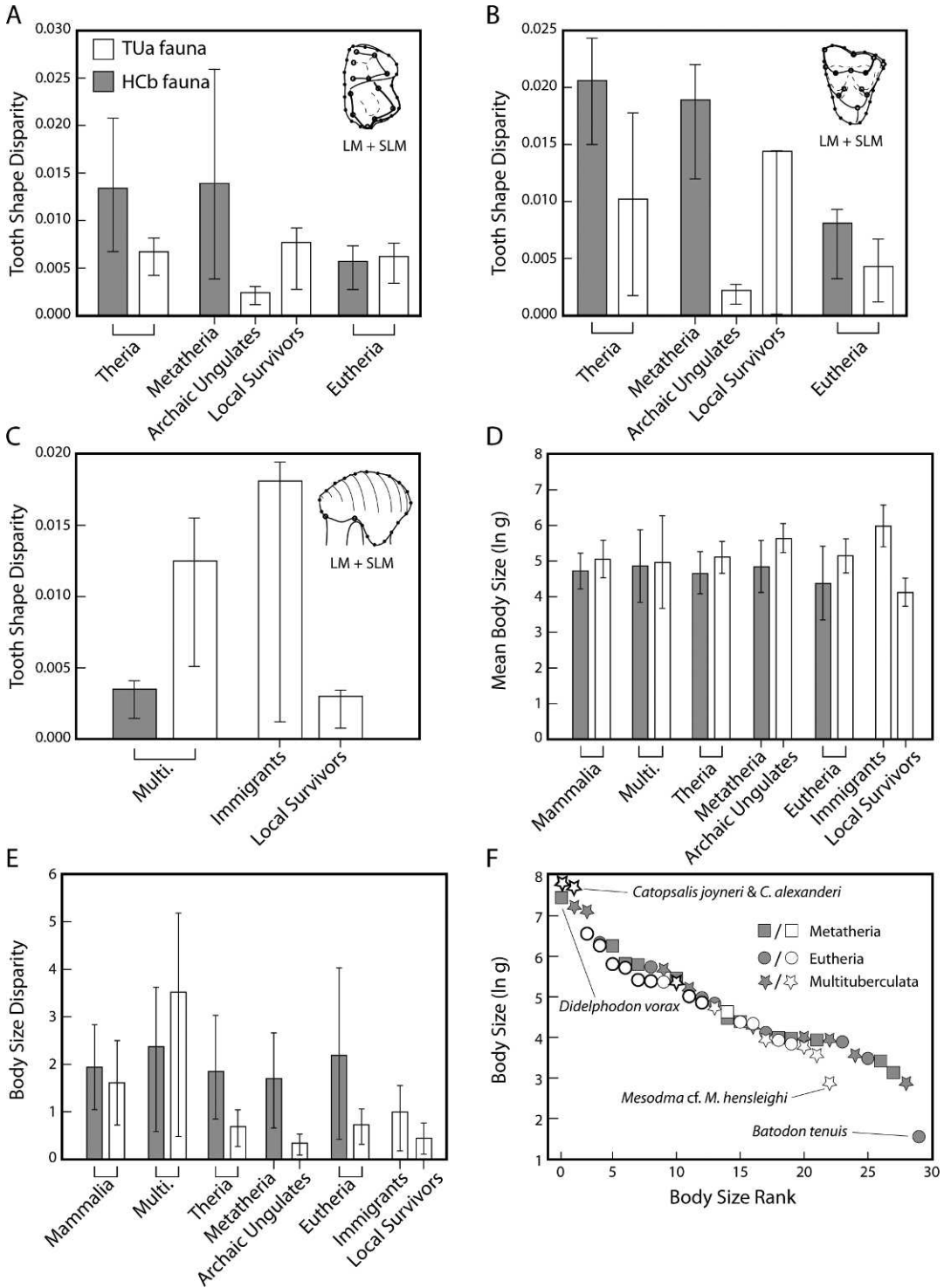


FIGURE 3. Dental-shape disparity values from geometric morphometric analyses of therian lower (A) and upper (B) molars, and multituberculate lower fourth premolars (C). Mean body size (D) and body-size disparity values (E) are from log-natural estimates of body masses. F, Plot of body-size vs. body-size rank for taxa in the HCb and TUa faunas. Values for the latest Cretaceous HCb fauna are represented as gray filled boxes and symbols and values for the earliest Paleocene TUa fauna as open boxes and symbols. Multituberculata is abbreviated as Multi. Immigrant taxa in F have symbols with greater stroke weight. Error bars represent 95% confidence intervals from species-based bootstrapping.

disparity of HCB therians. Note that two of five cimolestid species in the HCB fauna were not sampled in this analysis.

TUa Therians.—Archaic ungulates make up 57% of therian species in the TUa fauna but contribute less than 35% to the dental-shape disparity of TUa therians (Table 3). In the lower-molar analysis, the lone TUa metatherian, *Thylacodon montanensis*, has the highest partial disparity of any species (14.4%). The next highest contributions are from Leptictid sp. A (12.6%) and Palaeoryctid sp. A (12.1%). The leptictid (two species) and arctocyonid (five species) families have partial disparities of 22.3% and 20.5%, respectively, whereas peritychids (two species) contribute 7.7% to the lower-molar shape disparity of TUa therians.

In the upper-molar analysis, the partial disparities are highly skewed (Table 3). *Thylacodon montanensis* contributes 56.3%, the only sampled cimolestid (*Procerberus formicarum*) contributes 13.3%, and the seven species of archaic ungulates that were sampled contribute just over 30% to the upper-molar shape disparity of TUa therians.

Comparisons.—Group comparisons are shown in Figure 3A,B. The disparity values and significance values are in Supplementary Tables 4 and 5, respectively. Unless otherwise noted, statistical tests suggest that (1) for both lower-molar and upper-molar comparisons the observed differences in disparity are not the result of inadequate or variable specimen sampling (i.e., null hypothesis 1 rejected); (2) for upper-molar comparisons, observed differences in disparity could not be achieved from random sampling of a single pool of species (i.e., null hypothesis 2 rejected); but (3) for lower-molar comparisons, null hypothesis 2 could not be rejected.

Latest Cretaceous HCB therians, which consist of 20 species from nine families, have at least twice the dental-shape disparity of earliest Paleocene TUa therians, which consist of 14 species from seven families. The dental-shape disparity of the earliest Paleocene TUa local survivors is greater than that of the TUa therians as a whole (the immigrant taxa [archaic ungulates] are species-rich but morphologically conservative). Still, the dental-shape disparity of TUa local survivors is

considerably less than that of latest Cretaceous HCB therians. Null hypothesis 2 for the latter comparison was not rejected for either lower-molar or upper-molar values ($p = 0.48$, $p = 0.54$, respectively), although low sensitivity due to few degrees of freedom is likely a factor.

The dental-shape disparity of HCB metatherians is more than twice that of HCB eutherians and two to four times greater than that of earliest Paleocene TUa eutherians. Moreover, the disparity is significantly greater for HCB metatherians than for earliest Paleocene TUa archaic ungulates. Disparity was not calculated for TUa metatherians because they are represented by a single species (*Thylacodon montanensis*).

Dental-shape disparity in eutherians was relatively unchanged across the K/Pg boundary. In the lower-molar comparisons, the disparity of latest Cretaceous HCB eutherians is slightly less than that of earliest Paleocene TUa eutherians, but it is possible that the observed difference in disparity is the result of inadequate or variable specimen sampling ($p = 0.08$). In the upper-molar comparison, the disparity of HCB eutherians is almost twice that of TUa eutherians, but five of 13 TUa eutherians were not sampled in this analysis. The observed differences in lower-molar and upper-molar disparities are also achievable from random sampling of a single pool of species ($p = 0.80$, $p = 0.16$, respectively).

The dental-shape disparity of the TUa local survivors is two to six times greater than that of the TUa immigrants (archaic ungulates); however, note that four of six local survivors were not sampled in the upper-molar analysis. Nevertheless, it is unlikely that random sampling of a single pool of species could produce these differences in disparity for the lower-molar or upper-molar comparisons ($p = 0.003$, $p < 0.001$, respectively). Among the local survivors, the leptictid species and *Thylacodon montanensis* have very high partial disparities (49% and 21%, respectively).

Lower-Molar Morphospace Occupancy among Therians (Fig. 4, Supplementary Fig. 2)

In the PCA of the therian lower-molar data set, the first three axes explain 64.7% of the

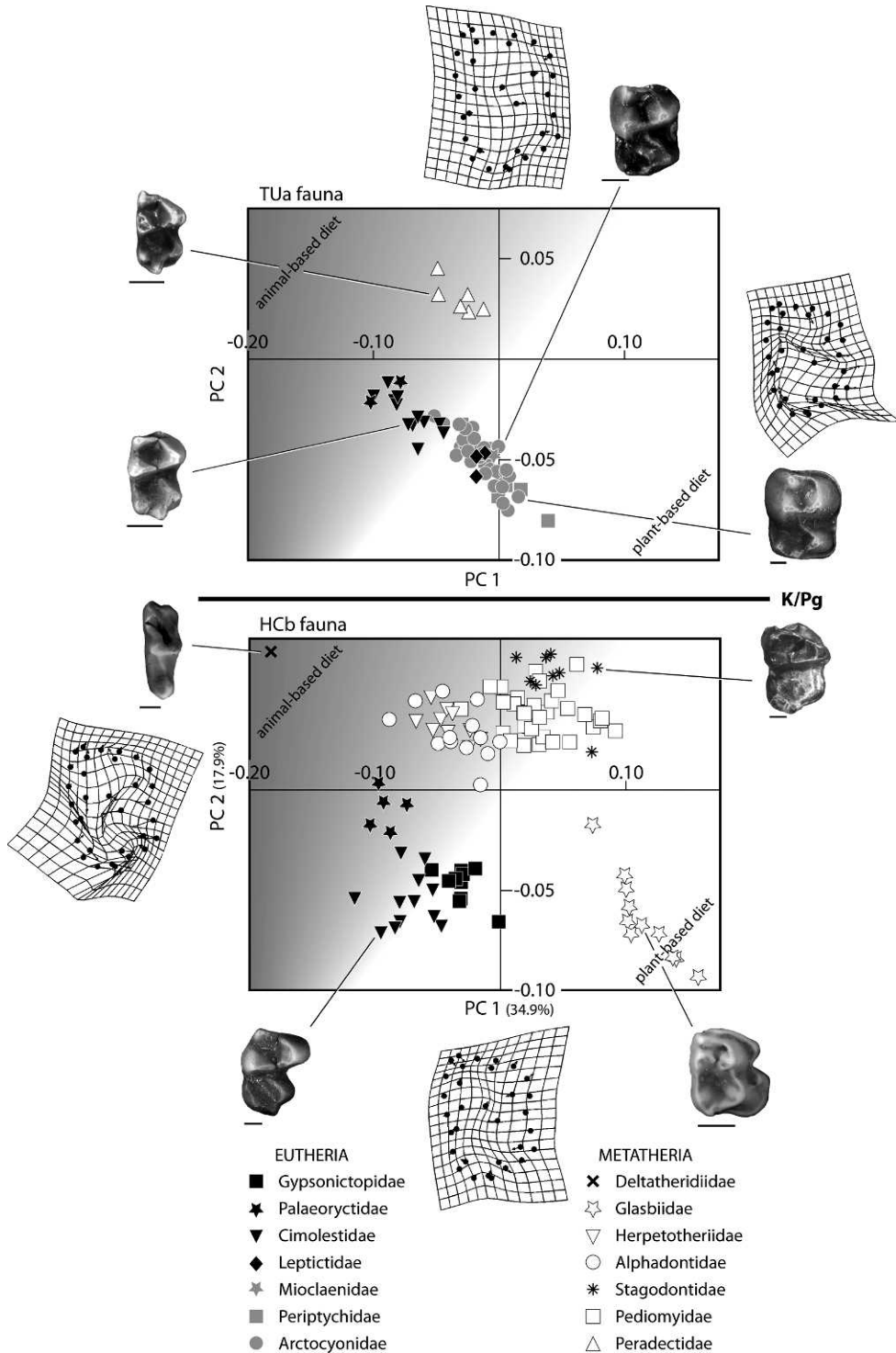


FIGURE 4. Lower-molar morphospace occupancy and relative shape changes of latest Cretaceous HCb (bottom panel) and earliest Paleocene TUa (top panel) therians from PCA of geometric morphometric data. The bivariate plot shows scores on PC1 and PC2, which explain 34.9% and 17.8% of the variance, respectively. Data points represent individual specimens. Open markers are for metatherians, black markers for local eutherians, gray markers for immigrant eutherians, and specific symbols for each family. The shaded gradient represents broad-scale interpretations of feeding

variance (Supplementary Table 6) and are significantly different in rank from one another. Figure 4 shows a bivariate plot of PC1 vs. PC2 scores of HCB therians (lower panel), PC1 vs. PC2 scores of TUA therians projected into the same morphospace (upper panel), deformation grids that represent the relative shape change at the extremes of each axis, images of exemplar specimens, and a shaded gradient representing broad-scale interpretations of feeding ecology. A bivariate plot of PC1 vs. PC3 is in Supplementary Figure 2.

Latest Cretaceous HCB metatherians from the Alphadontidae (3 species), Herpetotheriidae (*Nortedelphys jasoni*), Deltatheridiidae (*Nanocuris improvida*), and the earliest Paleocene TUA Peradectidae (*Thylacodon montanensis*) plot in the upper-left quadrant of the plot (Fig. 4). Most have weakly negative scores on PC1 and weakly positive scores on PC2; the deltatheridiid *Nanocuris improvida* has a strongly negative score on PC1 and a strongly positive score on PC2. Taxa in this quadrant are characterized by the following relative shape changes: (1) a mesiodistally and buccolingually expanded trigonid, (2) a mesiodistally elongate and buccolingually compressed talonid basin, (3) a more vertically oriented distal face of the trigonid, and (4) a more gracile, less inflated appearance at the base of the crown. Among the alphadontids, for example, these features are increasingly emphasized from *Turgidodon rhaister*, which plots closest to the origin, to *Alphadon marshi*, which plots more distally, and *Protalphadon foxi*, which plots most distally.

Latest Cretaceous HCB metatherians from the Pedomyidae (five species) and Stagodontidae (*Didelphodon vorax*) populate the upper-right quadrant of the plot (Fig. 4). None of the earliest Paleocene TUA therians are present in this quadrant. *D. vorax* tends to have higher scores on PC2 than the pedomyids do. Among the pedomyids, PC1 scores increase

from *Protolambda hatcheri* to *P. florencae*, *?Lep-talestes cooki*, *L. krejci*, and *Pedimys elegans*. Taxa in this quadrant are characterized by several relative shape changes: (1) a mesiodistally compressed trigonid, (2) a buccolingually expanded trigonid, (3) a buccolingually expanded talonid basin, (4) a buccally expanded base of the talonid, and (5) “twinning” of the entoconid and hypoconulid. Features 1, 4, and 5 are more pronounced along PC1, and feature 2 is more pronounced along PC2.

The HCB metatherian *Glasbius twitchelli* plots in the lower-right quadrant with strongly positive scores on PC1 and mostly strongly negative scores on PC2 (Fig. 4). Some specimens of earliest Paleocene TUA archaic ungulates (arctocyonids *Baiocodon nordicum*, *B. engdahli*, and *Oxyprimus erikseni*, and peripitychid *Mimatuta minuial*) also extend into this quadrant of the plot. They have weakly positive scores on PC1 and strongly negative scores on PC2 so do not overlap in space with *G. twitchelli*. Taxa in this quadrant are characterized by several relative shape changes: (1) a mesiodistally compressed trigonid, (2) a buccolingually compressed trigonid, (3) a greater mesial cant to the distal face of the trigonid, (4) a buccolingually expanded talonid basin, and (5) a buccally expanded base of the crown. Features 1 and 4 are more strongly expressed as scores increase along PC1.

With mostly negative scores on PC1 and negative scores on PC2, HCB and TUA eutherians fall almost entirely within the lower-left quadrant of the plot (Fig. 4). HCB gypsonictopids and TUA leptictids have weakly negative scores on PC1 and strongly negative scores on PC2, whereas HCB and TUA cimolestids have more strongly negative scores on PC1. HCB and TUA palaeoryctids have strongly negative scores on PC1 and weakly negative scores on PC2. Some TUA archaic ungulates (*Protungulatum donnae*) overlap in space with the HCB gypsonictopids

← ecologies from animal-based diets (gray) to plant-based diets (white). Deformation grids and vectors show the relative shape changes at the extreme of each axis. Images of right lower molars of HCB taxa are clockwise from the upper left: *Nanocuris improvida* (DMNH 55343), *Didelphodon vorax* (UWBM 91425), *Glasbius twitchelli* (UCMP 186601), and *Cimolestes magnus* (UA 3791). Images of TUA taxa are clockwise from the upper left: *Thylacodon montanensis* (UCMP 117792), *Oxyprimus erikseni* (UCMP 132350), *Baiocodon nordicum* (UMVP 1555), and *Procerberus formicarum* (UCMP 150001). Mesial is toward the top of the page. Scale bars, 1 mm.

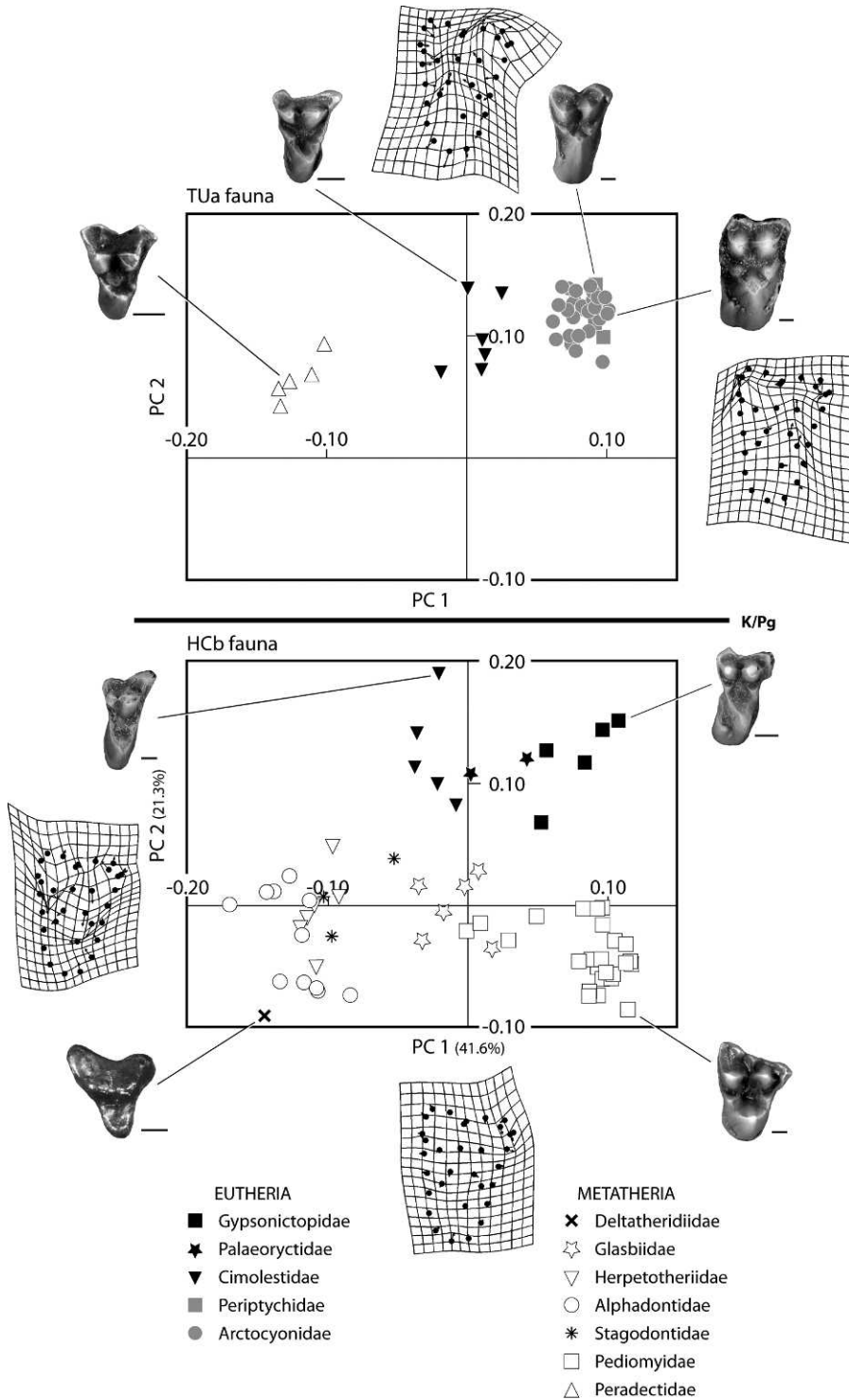


FIGURE 5. Upper-molar morphospace occupancy and relative shape changes of latest Cretaceous HCb (bottom panel) and earliest Paleocene TUa (top panel) therians from PCA of geometric morphometric data. The bivariate plot shows scores on PC1 and PC2, which explain 41.6% and 21.3% of the variance, respectively. Markers, symbols, and deformation grids are as in Figure 4. Images of upper right molars of HCb taxa are clockwise from the upper left: *Cimolestes stirtoni* (UMVP 3067), *Gypsonictops illuminatus* (UCMP 137304), *Protolambda florencae* (UCMP 186770), and *Nanocuris improvida*

as well, whereas others (*Protungulatum gorgun*) have more strongly negative scores on PC1, plotting among cimolestids. Still others (*Oxyprimus*, *Baiiconodon*, *Mimatuta*, mioclaenid sp. B) cross over into the lower-right quadrant of the morphospace. Taxa in this quadrant are characterized by (1) a mesiodistally expanded trigonid, in part due to the enlargement of the metaconid, (2) a buccolingually expanded trigonid, in part due to increased separation of the metaconid and protoconid, (3) inflated buccal and lingual bases of the trigonid and the buccal base of the talonid, (4) a buccolingually compressed talonid basin, and (5) a mesiodistally expanded talonid. Feature 3 is more pronounced as scores on PC2 become more strongly negative, whereas features 2 and 5 are more apparent as scores on PC1 become more strongly negative.

Upper-Molar Morphospace Occupancy among Therians (Figs. 5, 6)

In the PCA of the therian upper-molar data set, the first three PCs explain 74.8% of the variance (Supplementary Table 6) and are significantly different in rank from one another. Figure 5 shows a bivariate plot of PC1 vs. PC2 scores and Figure 6 shows a plot of PC1 vs. PC3 scores.

Latest Cretaceous HCB cimolestids have weakly negative scores on PC1 and strongly positive scores on PC2 (Fig. 5); the HCB alphadontid *Protalphadon foxi* has strongly negative scores on PC1 and weakly positive scores on PC2; and the earliest Paleocene TUa peradectid *Thylacodon montanensis* plots squarely in the upper-left quadrant with strongly negative scores on PC1 and strongly positive scores on PC2. Although a few specimens of the HCB herpetotheriid *Nortedelphys jasoni*, the stagodontid *Didelphodon vorax*, the glasbiid *Glasbius twitchelli*, and the TUa cimolestid *Procerberus formicarum* plot just inside the upper-left quadrant, the mean shape for each of those taxa falls in other quadrants. Taxa in the upper-left quadrant of

the plot are characterized by the following relative shape changes: (1) a transversely (buccolingually) expanded and mesiodistally compressed crown, (2) a buccally rather than distobuccally oriented postmetacrista, (3) an elongate preparacrista, and (4) metacone and metaconule small relative to the paracone and paraconule, respectively.

With weakly positive scores on PC1 and strongly positive scores on PC2, the latest Cretaceous HCB palaeoryctid *Batodon tenuis* and the earliest Paleocene TUa cimolestid *Procerberus formicarum* fall within the upper-right quadrant of the plot (Fig. 5). The HCB gypsonictopids and the TUa archaic ungulates, both of which have strongly positive scores on both PC1 and PC2, also plot in this quadrant. A specimen of *Glasbius twitchelli* plots just inside this quadrant but is considered elsewhere. Taxa in this quadrant are characterized by (1) a transversely expanded and mesiodistally compressed crown, (2) a reduced styler shelf and postmetacrista, (3) postmetaconule crista extending well beyond the metacone, and (4) a lingually expanded and enlarged protoconal base. Features 2 and 3 are less pronounced among the HCB palaeoryctids and the TUa cimolestids.

The lower-right quadrant of the plot (Fig. 5) is occupied by latest Cretaceous HCB pediomysids and a stray specimen of *Glasbius twitchelli*. The earliest Paleocene TUa therians are not present in this quadrant. Among the pediomysids, *Protolambda hatcheri*, *P. florencae*, and *?Leptalestes cooki* have strongly positive scores on PC1 and strongly negative scores on PC2; *Pedimys elegans* has strongly positive scores on PC1 and weakly negative scores on PC2; and *Leptalestes krejci* has weakly positive scores on PC1 and weakly negative scores on PC2. Taxa in this quadrant are characterized by (1) reduced transverse width of the crown, (2) greater mesiodistal length of the crown, particularly in the conular region, (3) a reduced parastylar region and preparacrista,

← (UCMP 137552). Images of TUa taxa are clockwise from the upper left: *Thylacodon montanensis* (UCMP 117770), *Procerberus formicarum* (UCMP 150010), *Mimatuta morgoth* (UCMP 132078), and *Baiiconodon nordicum* (UCMP 134693). Buccal is toward the top of the page. Scale bars, 1 mm.

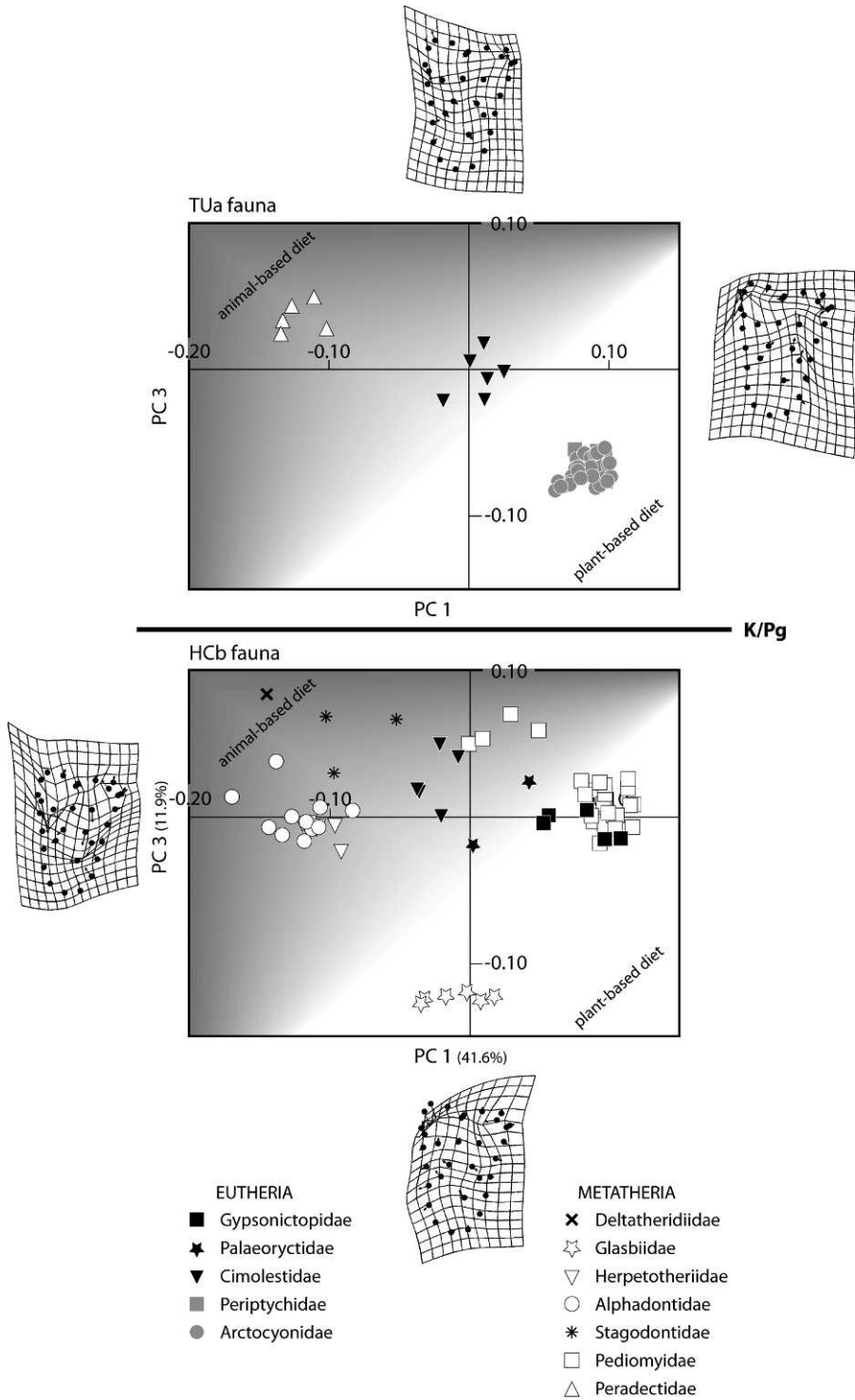


FIGURE 6. Upper-molar morphospace occupancy and relative shape changes of latest Cretaceous HCb (bottom panel) and earliest Paleocene TUa (top panel) therians from PCA of geometric morphometric data. The bivariate plot shows scores on PC1 and PC3; the latter explains 11.9% of the variance. Markers, symbols, shaded gradient, and deformation grids are as in Figure 4.

(4) elongate and distobuccally oriented post-metacrista and postmetaconule cristae.

Latest Cretaceous HCB alphadontids (except *Protalphadon foxi*), herpetotheriids (*Nortedelphys jasoni*), deltatheridiids (*Nanocuris improvida*), and stagodontids (*Didelphodon vorax*) plot mostly within the lower-left quadrant of the plot (Fig. 5). All of these taxa have strongly negative scores on PC1, and on PC2, *Nanocuris improvida* and the alphadontids *Alphadon marshi* and *Turgidodon rhaister* have strongly negative scores whereas *Nortedelphys jasoni* and *Didelphodon vorax* have weakly negative scores and a few positive scores. Earliest Paleocene TUA therians do not plot in this quadrant. The HCB taxa in this quadrant are characterized by (1) a broad styler shelf, particularly the metastyler region, (2) small conules, (3) a small protocone and protoconal base, and (4) a postmetaconule crista that terminates lingual to the metacone.

The latest Cretaceous HCB metatherian *Glasbius twitchelli* plots near the origin with weakly positive and weakly negative scores on both PC1 and PC2 (Fig. 5). Earliest Paleocene TUA therians are absent from this region of the morphospace.

Dental-Shape Disparity among Multituberculates (Table 4, Fig. 3C)

HCB Multituberculates.—The Cimolomyidae (*Meniscoessus robustus*, *Paressonodon nelsoni*, *Cimolomys gracilis*) contribute the most to p4-shape disparity of HCB multituberculates (55.6%; Table 4). The cimolodontid *Cimolodon nitidus* and the “*Paracimexomys*” group representative *Cimexomys minor* have partial disparities just over 10%, and the four species in the Neoplagiaulacidae have a combined partial disparity under 25%. Recall that the p4 of the distinctive cimolomyid *Essonodon browni* was not sampled in this analysis.

TUA Multituberculates.—The taeniolabidids *Catopsalis joyneri* and *C. alexanderi* and the microcosmodontid *Acheronodon garbani* contribute nearly two-thirds of the disparity of TUA multituberculates (Table 4). None of the other six TUA multituberculate species, including the morphologically distinctive eucosmodontid *Stygimys kuszmauli*, have a partial disparity over 10%.

Comparisons.—The p4-shape disparity of earliest Paleocene TUA multituberculates is more than three times greater than that of latest Cretaceous HCB multituberculates (Fig. 3C, Supplementary Table 4). This increase in disparity across the K/Pg boundary cannot be explained as inadequate or variable specimen sampling ($p < 0.05$) or random sampling of a single pool of species ($p < 0.01$). The earliest Paleocene TUA immigrants—the eucosmodontid *Stygimys kuszmauli*, the microcosmodontid *Acheronodon garbani*, and the taeniolabidids *Catopsalis joyneri* and *C. alexanderi*—have a p4-shape disparity that is greater than that of both the latest Cretaceous HCB multituberculates and the TUA local survivors. In both comparisons, null hypotheses 1 and 2 can be rejected (see Supplementary Table 5). HCB multituberculates, in turn, have greater p4-shape disparity than TUA local survivors of the K/Pg extinction event, but this difference in disparity could result from variable specimen sampling ($p > 0.05$) or from random sampling from a single pool of species ($p = 0.71$).

Dental Morphospace Occupancy among Multituberculates (Fig. 7, Supplementary Fig. 3)

In the PCA of the multituberculate p4 data set, the first three PCs explain 74.3% of the variance (Supplementary Table 6), and the relative ranks of the first two PCs are not statistically distinct from one another.

The latest Cretaceous HCB cimolomyid *Meniscoessus robustus* plots entirely within the upper-left quadrant (Fig. 7); it has strongly negative scores on PC1 and weakly positive scores on PC2. A few specimens from other HCB and TUA species plot within this quadrant, but because most specimens from these species plot in other quadrants, they are not discussed here. The taxa in this quadrant have p4s characterized by (1) a tall, mesiodistally compressed profile, (2) a mesiodistally expanded mesiobuccal lobe, and (3) a mesial aspect that slopes distodorsally.

Among the latest Cretaceous HCB multituberculates, the Cimolodontidae (*Cimolodon nitidus*), Neoplagiaulacidae (?*Neoplagiaulax burgessi*), and *Cimexomys minor* fall within the

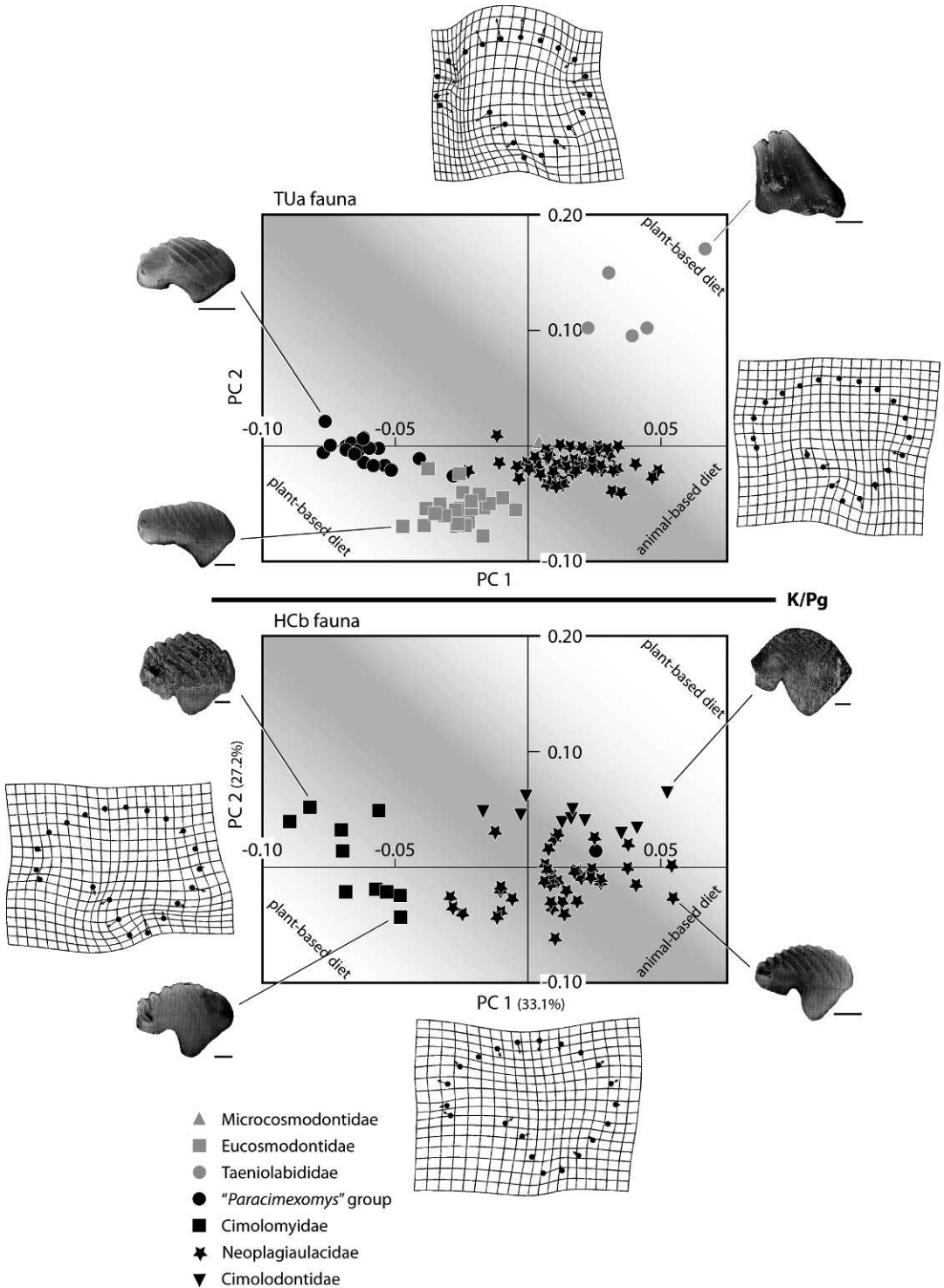


FIGURE 7. Lower-fourth-premolar morphospace occupancy and relative shape changes of latest Cretaceous HCB (bottom panel) and earliest Paleocene TUa (top panel) multituberculates from PCA of geometric morphometric data. The bivariate plot shows scores on PC1 and PC2, which explain 33.1% and 27.2% of the variance, respectively. Black markers are for local taxa, gray markers for immigrant taxa, and specific symbols for each family. The shaded gradient and deformation grids are as in Figure 4. Images of right lower fourth premolars of HCB taxa are clockwise from the upper

TABLE 3. Partial disparities (in %) for therian species and higher-level taxa in the HCb and TUa faunas based on analyses of lower-molar and upper-molar shape disparity for all therians in each of the faunas.

Partial Disparities of HCb therians			Partial Disparities of TUa therians		
	Lower molars (%)	Upper molars (%)		Lower molars (%)	Upper molars (%)
METATHERIA	69.7	68.5	METATHERIA	14.4	56.3
Deltatheridiidae	31.5	13.9	Peradectidae	14.4	56.3
<i>Nanocuris improvida</i>	31.5	13.9	<i>Thylacodon montanensis</i>	14.4	56.3
Stagodontidae	5.8	6.2	EUTHERIA	85.6	43.8
<i>Didelphodon vorax</i>	5.8	6.2	Arctocyonidae	20.5	19.6
Pediomyidae	15.1	22.5	<i>Protungulatum donnae</i>	2.4	2.9
<i>Pediomys elegans</i>	5.7	4.5	<i>Protungulatum gorgun</i>	3.0	2.8
? <i>Leptalestes cooki</i>	2.0	4.8	<i>Baioconodon engdahli</i>	4.3	4.1
<i>Leptalestes krejci</i>	3.2	2.0	<i>Baioconodon nordicum</i>	9.5	7.4
<i>Protolambda hatcheri</i>	2.0	5.5	<i>Oxyprinus erikseni</i>	1.3	2.4
<i>Protolambda florencae</i>	2.2	5.6	Periptychidae	7.7	10.9
Alphadontidae	5.4	16.1	<i>Mimatuta minuial</i>	3.7	7.4
<i>Protalphadon foxi</i>	3.1	5.5	<i>Mimatuta morgoth</i>	4.0	3.5
<i>Turgidodon rhaister</i>	1.0	5.1	Mioclaenidae	6.4	–
<i>Alphadon marshi</i>	1.4	5.5	Mioclaenid sp. B	6.4	–
Herpetotheriidae	1.5	3.5	Cimolestidae	16.5	13.3
<i>Nortedelphys jasoni</i>	1.5	3.5	<i>Cimolestes</i> sp. A	5.2	–
Glasbiidae	10.4	6.3	<i>Procerberus formicarum</i>	11.3	13.3
<i>Glasbius twitchelli</i>	10.4	6.3	Palaeoryctidae	12.1	–
EUTHERIA	30.4	31.4	Palaeoryctid sp. A	12.1	–
Gypsonictopidae	6.6	14.5	Leptictidae	22.3	–
<i>Gypsonictops hypoconus</i>	3.0	4.7	Leptictid sp. A	12.6	–
<i>Gypsonictops illuminatus</i>	3.6	9.8	Leptictid sp. B	9.7	–
Cimolestidae	21.0	12.8			
<i>Cimolestes stirtoni</i>	2.4	5.4			
<i>Cimolestes magnus</i>	5.0	3.9			
<i>Cimolestes cerberoides</i>	3.4	–			
<i>Cimolestes propalaeorcytes</i>	7.8	–			
<i>Cimolestes incisus</i>	2.5	3.5			
Palaeoryctidae	2.8	4.1			
<i>Batodon tenuis</i>	2.8	4.1			

upper-right quadrant (Fig. 7). *Cimolodon nitidus* and ?*Neoplagiaulax burgessi* have a range of weakly positive scores on PC1 with a few specimens that have weakly negative scores. On PC2, *Cimolodon nitidus* tends to have more strongly positive scores than ?*Neoplagiaulax burgessi*. From the TUa fauna, the taeniolabidids *Catopsalis joyneri* and *C. alexanderi* plot within this quadrant. With strongly positive scores on both PC1 and PC2, they do not overlap with *Cimolodon nitidus* or ?*Neoplagiaulax burgessi*. The p4s of the taxa in this quadrant are characterized by (1) a very tall, mesiodistally compressed profile, (2) a deep mesiobuccal lobe, (3) a symmetrical arc with

low mesial and distal ends, and (4) a sharp angle at the contact of the mesiobuccal lobe and the mesial aspect of the profile.

The neoplagiaulacid genus *Mesodma*, which is present in both the latest Cretaceous HCb fauna and earliest Paleocene TUa fauna, plots almost entirely within lower-right quadrant of the plot (Fig. 7). Most specimens have weakly positive scores on PC1 and weakly negative scores on PC2, but a few also extend into the lower-left quadrant with weakly negative scores on PC1. Individual species of *Mesodma* are not well separated from one another within this cluster. The TUa microcosmodontid *Acheronodon garbani* also plots within this

left: *Meniscoessus robustus* (UCMP 51507), *Cimolodon nitidus* (UCMP 50068), *Mesodma formosa* (UCMP 45726), and *Cimolomys gracilis* (UCMP 187778). Images of TUa taxa are clockwise from the upper left: *Cimexomys minor* (UCMP 111631), *Catopsalis joyneri* (UCMP 101000), and *Stygimys kuszmauli* (UCMP 92527). Mesial is to the right of the page. Scale bars, 1 mm.

TABLE 4. Partial disparities (in %) for multituberculate species and higher-level taxa in the HCb and TUa faunas based on analyses of lower-fourth-premolar shape disparity for all multituberculates in each of the faunas.

Partial Disparities of HCb multituberculates		Partial Disparities of TUa multituberculates	
	p4 (%)		p4 (%)
MULTITUBERCULATA		MULTITUBERCULATA	
Cimolodontidae	10.7	Neoplagiulacidae	15.2
<i>Cimolodon nitidus</i>	10.7	<i>Mesodma</i> cf. <i>M. hensleighi</i>	6.3
Neoplagiulacidae	23.6	<i>Mesodma</i> cf. <i>M. formosa</i>	4.1
<i>Mesodma hensleighi</i>	4.9	<i>Mesodma garfieldensis</i>	4.8
<i>Mesodma formosa</i>	7.2	Taeniolabididae	44.2
<i>Mesodma thompsoni</i>	4.6	<i>Catopsalis joyneri</i>	24.4
? <i>Neoplagiulax burgessi</i>	6.9	<i>Catopsalis alexanderi</i>	19.8
Cimolomyidae	55.6	Eucosmodontidae	7.5
<i>Cimolomys gracilis</i>	11.8	<i>Stygomys kuszmauli</i>	7.5
<i>Meniscoessus robustus</i>	22.2	Microcosmodontidae	22.0
<i>Essonodon browni</i>	-	<i>Acheronodon garbani</i>	22.0
<i>Paressonodon nelsoni</i>	21.6	" <i>Paracimexomys</i> " group	11.2
" <i>Paracimexomys</i> " group	10.4	<i>Cimexomys gratus</i>	5.4
<i>Cimexomys minor</i>	10.4	<i>Cimexomys minor</i>	5.9
<i>Paracimexomys priscus</i>	-		

quadrant. The p4s of taxa in this quadrant have (1) a low, distally elongate profile, (2) an asymmetrical arc, (3) a mesial aspect that is more vertical to convex, and (4) a deep mesiobuccal lobe that is mesiodistally compressed.

The lower-left quadrant of the plot (Fig. 7) is populated by the HCb cimolomyids *Cimolomys gracilis* and *Paressonodon nelsoni*, the TUa specimens of *Cimexomys minor* and *C. gratus*, and the TUa eucosmodontid *Stygomys kuszmauli*. A few specimens of the HCb and TUa genus *Mesodma* also plot in this quadrant. *Cimolomys gracilis*, *Paressonodon nelsoni*, *Cimexomys minor*, and *C. gratus* have strongly negative scores on PC1 and weakly negative scores on PC2, whereas *Stygomys kuszmauli* has weakly negative scores on PC1 and more strongly negative scores on PC2. Taxa in this quadrant have p4s with (1) a low, flattened profile that retains some of its height distally, (2) a mesial aspect that is low and convex, and (3) a shallow, distally shifted mesiobuccal lobe.

Mean Body Size and Body-Size Disparity (Fig. 3D–F)

Body sizes within the HCb fauna (Fig. 3F, Supplementary Table 2) range from the tiny shrew-sized eutherian *Batodon tenuis* (5 g) to the nearly raccoon-sized metatherian *Didelphodon vorax* (1.7 kg). In the TUa fauna (Fig.

3F, Supplementary Table 3), they range from the shrew-sized multituberculate *Mesodma* cf. *M. hensleighi* (18 g) to the woodchuck-sized multituberculate *Catopsalis joyneri* (2.4 kg). Mean body size is greater in the early Paleocene TUa fauna (157 g) than in the latest Cretaceous HCb fauna (112 g; Fig. 3D), but this difference is not statistically significant ($p = 0.39$). The TUa local survivors of the K/Pg event are very small (mean body size 61 g), significantly smaller ($p < 0.01$) than TUa immigrants (399 g; cf. tree squirrel 200–1000 g) but not the HCb fauna ($p = 0.18$).

The body-size disparity of the HCb fauna is slightly greater than that of the TUa fauna (Fig. 3E; $p = 0.33$) and significantly greater than that of the TUa local survivors ($p = 0.01$). The difference in body-size disparities between TU local survivors and TUa immigrants, however, is not significant ($p = 0.11$). The mean body sizes and body-size disparities of other major groupings are shown in Figure 3D and E, respectively. In all comparisons, the TUa group has a greater mean body size than the HCb group, but the differences are not statistically significant (Supplementary Table 5). In contrast, body-size disparities of the HCb groups are almost always greater than those of the TUa groups, but the differences are statistically significant only for HCb metatherians vs. TUa archaic ungulates and HCb eutherians vs. TUa eutherians.

The body-size structures (Fig. 3F) of the latest Cretaceous HCb fauna and the earliest Paleocene TUA fauna are very similar, despite high turnover across the K/Pg boundary. Both have (1) a slight gap between the largest-sized taxa ($>7.0 \ln g$) and the remainder of the taxa, (2) a shallow, continuous slope of medium-sized taxa, and (3) a precipitous drop at the smallest end of the body-size range. The distribution of body sizes among the TUA fauna also shows that the local survivors tend to be small bodied relative to the immigrants. *Acheronodon garbani*, an immigrant taxon not known by an m1 but with a very small p4, would be a counter example.

Discussion

Functional and Dietary Inferences

The functional and dietary inferences of the dental morphospaces that are presented below should be considered working hypotheses to be tested with additional lines of evidence (e.g., microwear, surface complexity, stable isotopes).

Therians.—The major functional axis of the lower-molar morphospace plot (Fig. 4, PC1 vs. PC2) extends from the upper-left corner (*Nanocuris improvida*) to the lower-right corner (*Glasbius twitchelli*). From the origin toward the upper-left corner, shearing capacity, particularly prevallid shearing, increases while crushing capacity decreases. In the opposite direction, from the origin toward the lower-right corner, prevallid and postvallid shearing are de-emphasized in favor of greater crushing capacity. The minor axis, which is orthogonal to the major axis, separates taxa by higher-level phylogeny in part. Metatherians are arranged toward the upper-right corner according to increases in both prevallid shearing capacity and crushing capacity, whereas eutherians are arranged toward the lower-left corner according to increased postvallid shearing and reduced crushing capacity. Higher axes were investigated (PC3–PC5), but they did not remove this phylogenetic signal or present a clear functional interpretation.

I interpret the major functional axis of the lower-molar morphospace (Fig. 4, PC1 vs. PC2), from the upper-left corner to the lower-

right corner, as a continuum of feeding ecologies from strict carnivory to animal-dominated omnivory and perhaps plant-dominated omnivory. The extreme ends of the minor functional axis are interpreted as strict carnivory and perhaps hard-object feeding in the upper-right corner, where the talonid basin is expanded to receive a broad protocone. On this basis, I infer that deltatheridiid *Nanocuris improvida* was a strict carnivore and, considering its estimated body mass (523 g; cf. slender-tailed meerkat 620–969 g), its diet likely included small vertebrates. Along this major axis—from *Protalphadon foxi* to *Nortedelphys jasoni*, *Thylacodon montanensis*, *Alphadon marshi*, and *Turgidodon rhaister*—feeding ecologies likely ranged from strict carnivory (mostly insects) to animal-dominated omnivory (insects, small vertebrates, fruits, seeds). The major axis ordines pediomysids from *Protolambda hatcheri* to *P. florencae*, *?Leptalestes cooki*, *Leptalestes krejci*, and *Pediomyis elegans*. On the minor functional axis, they are shifted higher than the alphadontids, herpetotheriids, and peradectids, which implies that in comparison pediomysids had increased shearing and crushing capacity and, by consequence, their diets were likely more omnivorous, though still largely animal based. The stagodontid *Didelphodon vorax* and the pediomysid *Leptalestes krejci* are even more extreme in their position on the minor functional axis, suggesting more carnivorous diets and perhaps hard-object feeding for the large-bodied stagodontid (1728 g; cf. European pine marten 800–1800 g). This inferred feeding ecology of *D. vorax* would be consistent with those based on functional interpretations of its bulbous premolars (Clemens 1966). *Glasbius twitchelli*, as indicated by its position in the lower-right corner of the morphospace, likely incorporated more plant matter (fruits, nuts, seeds, possibly leaves) into its diet than any other latest Cretaceous HCb therian did.

The distribution of eutherians along the major functional axis from palaeoryctids to cimolestids and gypsonictopids, leptictids, and archaic ungulates parallels that of metatherians from alphadontids to herpetotheriids, peradectids, and pediomysids. It suggests that the palaeoryctid *Batodon tenuis* was a strict

carnivore that, judging from its estimated body mass (4.72 g; cf. Eurasian shrew 5–14 g), probably ate only insects. The cimolestids were probably mostly carnivorous with little plant matter (fruits, seeds) in their diet. The large-bodied *Cimolestes magnus* (565 g; cf. slender-tailed meerkat 620–969 g) plots at the extreme end of the minor functional axis, implying a highly carnivorous diet comprising small vertebrates. The positions of gypsonictopids, leptictids, and archaic ungulates in the lower-molar morphospace lead to their ecological interpretation as animal-dominated omnivores. A few archaic ungulates, such as *Baiconodon nordicum* and *Mimatuta minui*, probably consumed substantially more plant matter.

The upper-molar morphospace plot of PC1 vs. PC2 (Fig. 5) appears to be a mix of functional and phylogenetic signals. Some functional separation is apparent on PC1: as scores become more positive, emphasis shifts from shearing features (e.g., elongate postmetacrista and preparacrista) to crushing features (e.g., enlarged protoconal region). In contrast, PC2 shows strong phylogenetic separation of metatherians with negative scores (e.g., transversely compressed crown, large metacone) and eutherians with positive scores (e.g., transversely expanded crown, large paracone). In exploring other axes, PC3 appears to lessen the phylogenetic signal of PC2 and ordines taxa by what appear to be largely functional features.

In the upper-molar morphospace plot of PC1 vs. PC3 (Fig. 6), the major functional axis extends from the upper-left corner (*Nanocuris improvida*), where shearing in the form of the preparacrista and postmetacrista is emphasized, to the lower-right corner (archaic ungulates, *Glasbius twitchelli*), where crushing is emphasized, as indicated by an enlarged protocone and protoconal base. Taxa in the lower-right corner are not without shearing; en echelon shearing is suggested by the postmetaconule crista that extends buccal to the metacone. The distribution of taxa along the major functional axis is very similar to that in the lower-molar morphospace (Fig. 4). Likewise, ecological interpretations of the upper-molar morphospace largely agree with

those from the lower-molar morphospace and are not further elaborated here.

Multituberculates.—The functional and ecological interpretations of p4 shape in the HCB and TUa multituberculates are informed by several studies: Krause (1982) detailed the functional role of the p4 of *Ptilodus* in the slicing-crushing cycle and the grinding cycle of mastication. Kielan-Jaworowska et al. (2004) outlined three major morphological associations of lower premolars and incisors and their functional implications. Wilson et al. (2012) showed that the ratio of molar:premolar length in multituberculates is positively correlated with cheek tooth row complexity (OPC), which is positively correlated with herbivory in living mammals (Evans et al. 2007). In turn, they inferred a diversity of dietary specializations among multituberculates, from carnivory to animal-dominated omnivory, plant-dominated omnivory, and high-fiber herbivory.

The p4 morphospace described by the PC1 vs. PC2 plot (Fig. 7) has a strong functional signal. The p4 that is characteristic of the upper-right quadrant close to the origin has a tall, arcuate profile and deep mesio Buccal lobe that is well suited for slicing large food items. The symmetrical nature of the profile also implies that the distal aspect of the p4 remained involved in the grinding cycle of mastication; that is, the molars, which generally have higher surface complexity and thus greater grinding capacity than a simple p4 blade, had not completely taken over the grinding function. Thus, it is likely that *Cimolodon nitidus* and *?Neoplagiaulax burgessi*, both of which plot in this region of the morphospace plot, were animal-dominated omnivores, rather than plant-dominated omnivores or strict herbivores, and possibly had diets that incorporated insects, fruits, seeds, and nuts. By comparison, the lower-profile, less symmetrical, and more distally elongate p4 that is characteristic of the lower-right quadrant has a less developed slicing capacity. The taxa that plot in this region of the morphospace, the HCB and TUa species of *Mesodma* and the TUa microsmodontid *Acheronodon*, likely had a dietary range from carnivory (insects) to animal-dominated om-

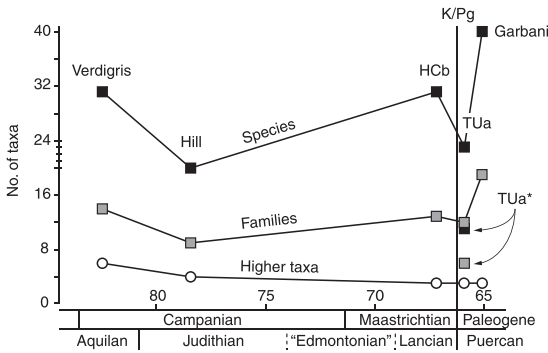


FIGURE 8. Late Cretaceous and earliest Paleocene patterns of taxonomic diversity (species, families, and supra-family taxa) in well-sampled, exemplar mammalian faunas. Data were compiled from the literature (see text). Age boundaries between NALMAs are based on Cifelli et al. (2004). Abbreviations: Verdigris, Verdigris Coulee fauna from the Milk River Formation in Alberta, Canada; Hill, Hill County fauna from the Judith River Formation in Hill County, Montana, U.S.A.; HCB, the HCB fauna from the upper part of the Hell Creek Formation in northeastern Montana; TUa, the TUa fauna from mostly the lowermost Tullock Formation in northeastern Montana (TUa* includes local survivors only, not immigrant taxa); and Garbani, the Garbani Channel fauna from the middle Tullock Formation in northeastern Montana.

nivory. In the left quadrants of the morphospace, the p4 profile is lower and less distally elongate than in the upper-right quadrant; functionally, the p4 may have had a reduced slicing capacity and a reduced role in the grinding cycle. Taxa in this region of the morphospace (*Cimolomys*, *Stygomys*, *Meniscoessus*) also have more elongate molars (molar: premolar length) and higher surface complexity (OPC; Wilson et al. 2012), all of which is consistent with the interpretation that taxa in this region of the morphospace had ceded most grinding responsibility to the molars and thus, had the grinding capacity to support plant-dominated herbivory to high-fiber herbivory. Among these taxa, *Meniscoessus robustus* had a taller, more mesiodistally compressed p4 profile with a larger mesio-buccal lobe, which may indicate that it still had significant slicing capacity and a strong animal-component to its diet. The most extreme morphological changes in the p4 are represented in the upper-right corner of the morphospace—mesiodistal compression of the crown, increased height of the profile, and near loss of the mesio-buccal lobe; these

are interpreted as a strong shift in p4 function, away from the typical multituberculate slicing-crushing cycle and toward a very reduced role in mastication. In combination with the enlargement of the molars and development of chisel-like incisors in *Catopsalis joyneri* and *C. alexanderi*, this leads to the inference that taxa in this region of the morphospace plot were high-fiber herbivores.

Ecomorphological Selectivity in the K/Pg Extinction

To better understand the diversity of the latest Cretaceous HCB fauna and the losses incurred in the K/Pg event, it is useful to put the latest Cretaceous HCB fauna into the context of older Late Cretaceous faunas of North America. Despite previous assertions that Cretaceous mammals were morphologically uniform (e.g., Alroy 1999), the ecomorphological diversity of older representative faunas has never been directly quantified other than via body size. In Figure 8, higher-level taxa serve as rough proxies for coarse comparisons among comparably well-sampled and well-studied faunas, acknowledging that explicit correction for what are likely minor differences in sampling intensity, area sampled, and paleoenvironment have not been applied. The Aquilan (?early Campanian) Verdigris Coulee fauna from the Milk River Formation in Alberta was as species rich as the HCB fauna but contained slightly more families and a greater number of higher-level taxa, particularly archaic mammal groups (eutricodontans, “symmetrodontans,” stem boreosphenidans; e.g., Fox 1971; Kielan-Jaworowska et al. 2004). The Judithian (late Campanian) fauna from the Judith River Formation in Hill County, Montana (Montellano 1992) had fewer species and families than the HCB and Verdigris Coulee faunas, but retained representatives of stem boreosphenidans in addition to multituberculates, metatherians, and eutherians. In this context, the HCB fauna was species rich, and, according to higher-level taxonomic proxies for ecomorphology, maintained a breadth of ecologies that was established in the Late Cretaceous and lasted until the K/Pg extinction.

The loss of mammalian taxa at the K/Pg boundary was substantial. Of the 28 mammalian lineages present in the upper 10 m of the Hell Creek Formation (a narrower stratigraphic interval than examined here) of northeastern Montana, 75% did not locally survive the K/Pg extinction in any form (e.g., daughter species); they either went extinct or emigrated outside of the Western Interior of North America (Wilson 2005, in press). Alroy (1999) found similar extinction rates from a regional database with coarser time bins (2.5 Myr). Although the breakdown of the affected taxa (91% of metatherians, 70% of multituberculates, 57% of eutherians) appears lopsided, Wilson (in press) rejected the hypothesis of taxonomic selectivity among mammals. Meanwhile, few studies have directly quantified ecomorphology and tested for ecological selectivity in the K/Pg extinctions. Borths and Hunter (2008) used a sample of ulnae across the K/Pg boundary to evaluate the Robertson et al. (2004) hypothesis that survivors would have had to seek shelter below ground or underwater to avoid the proposed secondary effects of the bolide impact (e.g., thermal pulse). Although Borths and Hunter (2008) found no evidence of mammalian survivors with burrowing or aquatic specializations, their functional interpretations indicated greater locomotor diversity among Lancian taxa than previously expected; for example, the stagodontid metatherian and K/Pg victim *Didelphodon vorax* was possibly semiaquatic. Using a global data set partitioned into 5-Myr temporal bins, Wilson et al. (2012) showed that disparity in dental complexity and body size in multituberculates increased during the Late Cretaceous and was undiminished across the K/Pg boundary. Their dietary interpretations of the dental-complexity data suggest that the breadth of multituberculate feeding ecologies (insectivores, omnivores, herbivores) was not selected against in the K/Pg extinction.

Here I have investigated dental (dietary) ecomorphology and body size across the boundary for entire mammalian communities within an ecosystem. The latest Cretaceous HCB fauna had a modest range of inferred body sizes, from a shrew-sized eutherian to a

raccoon-sized metatherian, whereas inferred feeding ecologies likely ranged from a few specialized carnivores to more than a handful of plant-dominated omnivores and high-fiber herbivores among a large diversity of carnivores and animal-dominated omnivores. The metatherians covered much of this range in body size and feeding ecology. In contrast, eutherians had a similar span of body sizes, but had not exploited the plant-dominated omnivory to high-fiber herbivory end of the dietary spectrum. Although multituberculate morphological disparity values are not directly comparable with therian values, the spectrum of body sizes and inferred feed ecologies indicate that multituberculates were as ecologically diverse as metatherians or more so.

In the context of massive losses of species and higher-level mammalian taxa across the K/Pg boundary—the number of families dropped by 53.8% from 13 HCB families to six families among the TUA local survivors (TUA* in Fig. 8)—a corresponding drop in ecomorphological diversity might also be expected. However, taxonomic and ecological severities of extinctions are not necessarily coupled (McGhee et al. 2004). A case in point is that, among the “big five” mass extinctions, the continental K/Pg event is ranked last in taxonomic severity (6.3% family-level extinction [Benton 1995]), but because it triggered the collapse of dinosaur-dominated ecosystems, it and the end-Permian event were qualitatively ranked highest in ecological severity (McGhee et al. 2004). Direct comparison of taxonomic and ecomorphological severities indicates that declines in ecomorphological diversity of mammals across the K/Pg boundary in northeastern Montana were relatively modest. Among therians, the local disappearance of 78% of species across the K/Pg boundary (Wilson 2005, in press) was accompanied by drops of 42.5% and 30.1% in dental-shape disparity (lower molars, upper molars, respectively). These declines in disparity do not appear to be due to specimen-sampling error, but the role of species-sampling error cannot yet be ruled out. It should be noted that with only six local survivors, the permutation test (or an *F*-test) is more prone to Type II error (failure to reject a false null

hypothesis). If the observed reductions in disparity are taken at face value, they imply that the culling of ecomorphological diversity was nonrandom with respect to molar morphology and, by proxy, feeding ecology. Instead of an even thinning of morphospace, which would have left disparity unchanged, some areas of the dental morphospace were disproportionately affected. In the lower-molar morphospace, the lower-right and upper-right quadrants were emptied and the upper-left quadrant was thinned. In the upper-molar morphospace, the lower-left and lower-right quadrants were emptied. Although five TUA eutherian species are missing from the upper-molar analysis, it is highly unlikely that they would plot in the vacated quadrants, given their family assignments and lower-molar morphology. Thus, the extinctions seem to have removed ecological end-members of the HCB fauna, such as specialized carnivores (e.g., *Nanocuris improvida*, *Didelphodon vorax*, *Cimolestes magnus*) and plant-dominated omnivores (*Glasbius twitchelli*), and heavily thinned a substantial diversity of carnivores and animal-dominated omnivores (e.g., alphasodontids). Among multituberculates, p4-shape disparity remained largely intact across the K/Pg boundary. The disappearance of 70% of multituberculate species translated to a loss of only 14.3% in p4-shape disparity. Tests of significance cannot rule out the role of either specimen-sampling error or species-sampling error. Moreover, the extinctions left no major areas of the dental morphospace empty. The extinctions of *Mensiscoessus robustus*, *Cimolomys gracilis*, *Cimolodon nitidus*, and *?Neoplagiaulax burgessi*, for example, only trimmed the edges of the occupied morphospace (Fig. 7), which represent more specialized animal-dominated omnivory, plant-dominated omnivory, and herbivory.

Body-size disparity also significantly decreased across the K/Pg boundary (HCB Mammalia vs. TUA local survivors, Supplementary Table 5), indicating that the loss of taxa was nonrandom with respect to body size. Alroy (1999: p. 116) stated, "there was an abrupt shift in the mean [body mass] just around the K-T boundary, which resulted from the extinction of many small mammals

and the addition of many medium-sized mammals." In my study, a decrease in mean body mass across the K/Pg boundary from 112 g (HCB Mammalia) to 61 g (TUA local survivors) is nonsignificant ($p = 0.18$). However, logistic regression of body size and survivorship in HCB mammals indicates that smaller body size significantly predicts lineage survivorship (-1.68 size coefficient, $p = 0.02$; Supplementary Appendix 2), implying that there was extinction selectivity against larger-bodied mammals across the K/Pg boundary. This pattern is consistent with some previous studies of vertebrates (Archibald 1996; Fara 2000; see below), but was not recovered for mammals by Alroy (1999), perhaps because his study used larger temporal bins or did not discriminate between survivors and immigrants, or simply because the pattern is localized to northeastern Montana.

In sum, mammalian taxa of larger body size and more-specialized feeding ecologies were more severely hit by the K/Pg extinction event, whereas smaller-bodied, less specialized carnivores and animal-dominated omnivores had a better chance of survival. Alternatively, this apparent pattern of selectivity might to some degree reflect sampling (Jablonski 2005). For example, there are fewer plant-dominated omnivores and herbivores than carnivores and animal-dominated omnivores in the HCB fauna; thus, they may simply have had fewer chances to survive the K/Pg extinction event. Parallel study of mammalian communities in other areas (e.g., Alberta, North Dakota, Colorado) will continue to test the generality and, thus, the statistical significance of these patterns.

What bearing do these patterns of extinction and survival of mammals in northeastern Montana have on the debate over selectivity in mass extinction? Lupia (1999), having found no drop in morphological disparity of angiosperm pollen across the K/Pg boundary, concluded that the extinction event was nonselective in terms of the measured traits of angiosperm pollen. Jablonski and others (Jablonski 1986, 2005; Jablonski and Raup 1995; Lockwood 2004, 2005) found nonrandom patterns of extinction among end-Cretaceous bivalves, which led them to conclude

that nonconstructive selectivity was in operation. That is, traits that were adaptive in background times (e.g., body size, life position, trophic strategy, species richness) did not correlate with K/Pg survivorship, whereas other traits that were not especially adaptive in background times (broad geographic range at the genus level; but see Payne and Finnegan 2007) enhanced survivorship during the K/Pg mass extinction event.

The pattern of extinction among mammals in northeastern Montana appears to be non-random with respect to inferred diet and body size, and the victimized traits (larger body size, more specialized diet) are ones that correlate with extinction vulnerability in modern and background extinctions. Thus, in contrast to a mass extinction regime of either nonselectivity or nonconstructive selectivity, the mammalian pattern suggests a process of constructive selectivity across the K/Pg boundary. Patterns of constructive selectivity are not as unusual for the K/Pg extinction (McKinney 1997) as opposing claims might imply (Jablonski 2005). In the marine realm, K/Pg survivorship is correlated with smaller body sizes in planktonic foraminifera (Norris 1991) and with feeding strategy in sea urchins (Smith and Jeffery 1998). In scleractinian corals, reliance on photosymbiosis and coloniality (as well as narrow geographic range) were associated with greater extinction risk at the K/Pg boundary; however, other traits that are expected to confer extinction resistance, such as abundance, species richness, larval feeding mode, and skeleton size, were not correlated with survivorship (Kiessling and Baron-Szabo 2004). In the terrestrial realm, Archibald (1996: Fig. 8.11) analyzed extinction patterns in a large vertebrate fossil database from northeastern Montana (updated from Archibald and Bryant 1990). Although levels of statistical significance were not provided, K/Pg survivorship was greater in smaller-bodied species (under 25 kg) vs. larger-bodied species, ectotherms vs. endotherms, non-amniotes vs. amniotes, and aquatic vs. terrestrial species (see also Sheehan and Fastovsky 1992). Analyzing a global database of tetrapod families with coarse ecological assignments, Fara (2000) also found evidence of diet-

habitat-, and size-selectivity across the K/Pg boundary, wherein families of small omnivores and invertebrate-eaters that were dependent on freshwater or humus habitats fared better than families of large herbivores and tetrapod-eaters that were based in terrestrial habitats.

What remains unclear is (1) how broadly these patterns of selectivity apply across taxonomic groups and geographic regions and (2) whether these traits directly affected survivorship or whether they are simply correlates of other factors (Levinton 1996; Jablonski 2005). If other traits, such as geographic range above the species level, more directly influenced survivorship, then the apparent pattern of constructive selectivity would be more accurately interpreted as nonconstructive selectivity. Among K/Pg mammals, it has yet to be tested whether body size and feeding ecology correlate with other factors, such as abundance and geographic range. A full-scale analysis of these factors is beyond the scope of this study, but published genus- and species-level geographic ranges (Hunter and Archibald 2002) and abundance data of HCb taxa (Wilson 2005, in press) do not readily support these as contributing factors. Also note that Vilhena and colleagues (2012) recently used network methods to reanalyze the global bivalve data set of Raup and Jablonski (1993) that was originally used to support the case for nonconstructive selectivity across the K/Pg boundary; they found that geographic range was in most cases not as strong a predictor of survivorship as membership in specific biogeographically organized, biome-level units.

Examples of constructive selectivity across the K/Pg boundary appear inconsistent with arguments that a major, globally instantaneous, catastrophic kill mechanism would produce a nonselective pattern of extinction (Archibald 1996; Villier and Korn 2004). However, Robertson et al. (2004) hypothesized that an intense, overhead infrared thermal pulse sweeping across the globe in the first few minutes to hours following the K/Pg impact could explain nonrandom patterns of extinction among nonmarine vertebrates (but

see Goldin and Melosh 2009 for a model that predicts a less severe thermal pulse). Robertson et al. (2004) suggested that individuals with sheltering behavior, either underground or underwater, or that were “small enough to shelter in soils, deep in rock piles, or possibly in holes in very large trees” (p. 764) would have had a higher probability of initial survival. The thermal-sheltering hypothesis, while compelling and consistent with some broader taxonomic patterns, provides little power to predict fine-scale extinction patterns among what are all relatively small-bodied mammals. Instead, mammals may largely have passed through this filter, if it existed, and been affected more by longer-term environmental perturbations resulting from major pulses of volcanism during the 300–500 Kyr leading up to the K/Pg boundary (Chenet et al. 2009), temporary disruption of primary productivity potentially brought on by the K/Pg impact (Alvarez 1986), or both. The pattern of ecomorphological selectivity among K/Pg mammals in northeastern Montana, for example, is more consistent with the hypothesis proposed by Sheehan and Hansen (1986), in which taxa that relied upon plant-based food chains (herbivores) would have been selected against whereas taxa independent from primary productivity in detritus-based food chains (insectivores, omnivores) would have been buffered from extinction (also Buffetaut 1984; Sheehan and Fastovsky 1992; Janzen 1995; Sheehan et al. 1996; but see Levinton 1996 for a critique of the parallel to this hypothesis in the marine realm). Quantitative ecomorphological studies of extinction patterns in small-bodied amphibians and lizards, for example, would provide additional tests of this hypothesis.

Filling Ecomorphological Space in the K/Pg Survival Fauna

The TUA fauna, a mammalian community in the immediate aftermath of the K/Pg extinction event, offers an opportunity to examine the filling of ecomorphological space within an ecosystem during the earliest phase of the K/Pg recovery, when the stage would be set for the Paleocene evolutionary radiation of placentals (Van Valen 1978; Alroy 1999).

The earliest Paleocene (Pu1) TUA fauna was species-poor relative to typical latest Cretaceous faunas and subsequent “recovery faunas,” such as the Pu2/3 Garbani Channel Quarry (Fig. 8) (Clemens 2002; Wilson in press), concordant with patterns commonly observed for faunas in the “survival” stage of recoveries (sensu Erwin 1998). Among the local survivors (and their descendant species), a few taxa predominated (*Procerberus formicarium*, *Mesodma thompsoni*, *Thylacodon montanensis* [Wilson in press]) and may have thrived in difficult environmental conditions (i.e., “bloom” taxa). There was also an influx of immigrant taxa (>50% of TUA species) into the study area during or immediately after the K/Pg event, although the relative abundance of the immigrants was low (<15% of TUA individuals). This pattern is consistent with results from neoecological studies of diversity-invasibility (Levine and D’Antonio 1999) and suggests that in situ speciation was less important for the initial taxonomic recovery of mammalian communities following the extinction (see below).

Whereas higher-level taxonomic proxies suggest that the ecomorphological diversity of the TUA fauna, which consists of immigrants and local survivors, was slightly depressed relative to Late Cretaceous faunas (Fig. 8), direct quantification of ecomorphological diversity provides mixed signals. Across the K/Pg boundary, dental-shape disparity decreased in therians and increased in multituberculates, whereas mean body size and body-size disparity did not significantly change. As was the case with taxonomic recovery, in situ ecomorphological diversification was minimal during the survival interval, and the initial filling of ecospace largely resulted from the influx of immigrants. For example, although large-bodied HCB taxa were selectively culled at the K/Pg boundary, mean body size was maintained across the K/Pg boundary almost entirely by the arrival of TUA immigrants, which had a significantly higher mean body size (399 g) than the TUA local survivors did (61 g; $p < 0.01$).

In terms of dental-shape disparity, the multituberculate immigrants (Taeniolabidae, Eucosmodontidae, Microcosmodontidae)

made a significant contribution to the TUA fauna (TUA multi immigrants > TUA multi local survivors; $p < 0.01$). The taeniolabidid *Catopsalis* species occupy the upper-right corner of the p4 morphospace, distant from all other taxa (Fig. 7), and the eucosmodontid *Stygmymys kuszmauli* fills an area in the lower-left quadrant, adjacent to the area previously filled by *Cimolomys gracilis* and *Paressonodon nelsoni*. As inferred above, these newly populated regions of the morphospace correspond to high-fiber herbivory and plant-dominated omnivory, respectively. *Acheronodon garbani* plots among species of *Mesodma* in a well-colonized area of the morphospace that corresponds to animal-dominated omnivory.

The contribution of therian immigrants to the TUA fauna differed strongly from that of multituberculate immigrants. All eight species of therian immigrants are archaic ungulates, albeit spread across three families (Arctocyonidae, Peripitychidae, Mioclaenidae). The dental-shape disparity added by the archaic ungulates did not exceed that contributed by the TUA therian local survivors ($p < 0.01$). The dental morphospace occupancy (Figs. 4–6) best illustrates this point, showing a tight cluster formed by taxonomically diverse but morphologically similar archaic ungulates. As Lillegraven and Eberle (1999: p. 702) suggested, Pu1 archaic ungulates have “similar, generalized dentitions” and “probably did not vary greatly in niche requirements.” Notably, however, this tight cluster stretches into regions of the morphospace that were not colonized or not heavily colonized by latest Cretaceous HCB therians; some are near regions of the morphospace that were previously occupied by *Gypsonictops* spp., *Glasbius twitchelli*, and some pediomyid metatherians. The inferred dietary spectrum of the archaic ungulate immigrant taxa ranges from animal- to plant-dominated omnivory. Thus, immigration into the study area served a critical role in the initial recovery process, infusing an otherwise depleted TUA survival fauna with taxonomic and ecomorphologic diversity (see Clemens 2010 for further discussion of the contributions of immigrants to K/Pg recovery). It follows that evolutionary diversification of archaic ungulate and multituberculate

immigrants must have begun in the latest Cretaceous in regions outside the study area (Lillegraven 1969; Archibald 1982; Fox 1989). If so, additional questions arise, such as, What was the tempo and pattern of mammalian evolution in the source area or areas for these immigrants? What factors triggered the evolution of these taxa in the source area or areas and allowed their survival across the K/Pg boundary? Had non-avian dinosaurs gone extinct earlier in these other areas or imposed less severe constraints on mammalian evolution? Where and under what circumstances were mammalian taxa with at least partially plant-based diets able to survive the K/Pg extinction event? Continued fieldwork in areas outside the northern Western Interior will help clarify these and other important issues.

Archibald (1983, 1996) hypothesized that the near-complete regional extinction of metatherians resulted from direct competition with archaic ungulates. Hunter (1997) tested this hypothesis by examining patterns of relative abundances, body size, locomotion, and dental morphology of archaic ungulates and metatherians through latest Cretaceous and early Paleocene of North America. His traditional morphometric analysis of molar morphology revealed broad overlap of these taxa in his morphospace, a necessary precondition if these taxa directly competed for food resources. Overall, though, he found little support for Archibald’s hypothesis, but qualified his interpretations in light of uncertainties in the ages of some localities at the time of his study. The results from my geometric morphometric analysis, which are framed within a high-precision local chronostratigraphy, are also consistent with some overlap in morphospace and inferred similarity in feeding ecology among archaic ungulates and some metatherians, particularly *Glasbius* and some pediomyids. However, as Hunter (1997) noted, these taxa have never been convincingly shown to coexist in the local study area. Most reports of their co-occurrence in north-eastern Montana or elsewhere are either unconfirmed (Breithaupt 1982) or now believed to be the result of reworked Lancian metatherian fossils in Puercan-age channel

deposits (Lofgren 1995; see also Cifelli et al. 2004). The Spigot Bottle local fauna in Carter County, southeastern Montana, provides the only conclusive evidence that archaic ungulates and latest Cretaceous metatherians ever coexisted (Archibald et al. 2011). The Spigot Bottle fossil assemblage contains nearly 1200 specimens, of which there is only one archaic ungulate specimen (0.08% relative abundance) compared with 374 metatherians (31.27%). Even in the earliest Paleocene (Puercan), in which archaic ungulates were taxonomically diverse, they were not numerically abundant. They account for less than 12% of all mammal specimens in both early (Pu1) and later Puercan (Pu2/3) assemblages of northeastern Montana (Wilson in press); only by the early Torrejonian (To1), approximately 1 Myr after the K/Pg extinction, had archaic ungulates become both taxonomically (50% of species) and numerically abundant in the local section (29% relative abundance [Wilson in press])—hardly the “double wedge” pattern predicted by a competitive exclusion scenario (Benton 1987, 1991). This lag between richness and relative abundance is also in conflict with the model of incumbent replacement (Rosenzweig and McCord 1991), in which rates of competitive speciation and ecospace filling are proportional to the rate of extinction. Rather than a competitive exclusion scenario or a rapid replacement scenario, a more accurate interpretation of the available data is a gradual opportunistic replacement of some latest Cretaceous metatherians by archaic ungulates, ramping up over 1 Myr (Benton 1983). Whereas the narrow ecomorphological breadth of earliest Paleocene (Pu1) TUa archaic ungulates could be said to be consistent with the label of nonadaptive radiation given by Archibald (2011), Lillegraven and Eberle (1999) noted a qualitative increase in the morphological diversity of archaic ungulates at the Pu1–Pu2 transition in the Ferris Formation of the Hanna Basin, south-central Wyoming. Likewise, I suspect that quantitative analysis of the Garbani Channel local fauna (Pu2/3) would find an equal if not greater increase in morphological diversity of archaic ungulates by this point in the local section; thus, I would agree with Hunter

(1997) that the diversification of archaic ungulates was an adaptive radiation, albeit somewhat delayed relative to the K/Pg extinction (Erwin 1992).

Qualitative assessment of the Garbani Channel local fauna, which is from ~600–900 Kyr after the K/Pg boundary (Pu2/3 interval), also supports the idea that a broader adaptive radiation of placental mammals began within the first 400 Kyr to 1 Myr of the Paleocene. The Garbani Channel local fauna thus far consists of 40 recognized species (Clemens 2002; Wilson in press) that record a broad range of inferred feeding ecologies, from specialized carnivores to omnivores, high-fiber herbivores, and rooters, and body sizes that ranged up to a badger-sized taeniodont (cf. *Wortmania* [Clemens 2013]) and triisodontid eutherians (*Eoconodon* cf. *E. guadrianus* 3.7 kg), and a nearly beaver-sized multituberculate (*Taeniolabis lamberti* 11.0 kg). Sampling of faunas in the 35–40 m stratigraphic gap between the TUa fauna and the Garbani Channel local fauna will further resolve the timing and pattern of changes leading up to the adaptive radiation of placental mammals. Regardless, it is clear that there was significant lag time between the extinction of non-avian dinosaurs and the filling of the vacated ecospace.

Conclusions

The association between the extinction of non-avian dinosaurs in the K/Pg event and the rise of placental mammals has become conventional wisdom. Temporally, geographically, and ecologically coarse studies bear this pattern out (Lillegraven 1972; Alroy 1999), but quantitative ecomorphological analyses at fine temporal and geographic scales are few. This study focused on a single area, northeastern Montana, and mammalian paleocommunities immediately before and after the K/Pg extinction event. It benefited from a well-constrained chronostratigraphic framework, well-sampled and well-studied fossil assemblages, and ecomorphological inferences from quantitative dental data. The results of this ecosystem-level view of the K/Pg extinction and initial stage of recovery in the study area provide several insights that may apply more broadly:

1. Cretaceous mammalian faunas are often regarded as taxonomically depauperate and morphologically uniform relative to Paleocene faunas (e.g., Alroy 1999; but see Luo 2007 and Wilson et al. 2012). Dental-shape data from this study imply that this portrayal has been somewhat overstated. Latest Cretaceous metatherians and multituberculates, in particular, had a broader range of inferred diets than often perceived, from the carnivorous deltatheridiid *Nanocuris* to taxa with more plant-based diets, including *Glasbius* and some multituberculates, such as *Cimolomys* and *Meniscoessus*.
2. The ecomorphological losses across the K/Pg boundary were moderate, particularly for multituberculates, despite severe taxonomic losses particularly for metatherians. Nevertheless, the pattern of losses points to ecological selectivity against taxa of larger body size and with diets dependent on primary production (carnivory, herbivory). This nonrandom pattern implies that the kill mechanism for at least mammals was not as globally instantaneous and devastating as a thermal pulse (Buffetaut 1990) but more likely a disruption in primary productivity from environmental perturbations resulting from massive volcanism or from prolonged darkness of an impact dust cloud.
3. The ecomorphological diversity of the TUA mammalian fauna across the K/Pg boundary was not immediately stoked by ecological release from non-avian dinosaurs. Instead, in the wake of significant mammalian taxonomic and ecomorphological losses in the K/Pg event, speciation and ecomorphological diversification lagged in the earliest Paleocene, and the initial ecomorphological replacement and modest expansion of mammals were almost entirely due to an influx of multituberculate and archaic ungulate immigrants. The multituberculates expanded further into herbivore ecomorphospace through the addition of taeniolauidids. Archaic ungulates, despite great taxonomic richness, filled a narrow but previously underpopulated region of the ecomorphospace (animal- and plant-based omnivory) that was in part previously occupied by some metatherians. Overall, the pattern reflects a delayed opportunistic replacement rather than a competitive exclusion scenario.
4. Qualitative data from the study area indicate that within 1 Myr of the K/Pg boundary, the adaptive radiation of placentals was well underway. Quantifying the ecomorphological diversity of younger mammalian faunas from the study area (e.g., Garbani Channel local fauna) will refine this local pattern, and expanding this approach to other geographic areas in the Western Interior (and outside of North America) will begin to document the geographic variation of the extinction and recovery patterns that is so often overlooked (Buffetaut 1990; Jablonski 1998). For example, the surprisingly diverse late Pu1 Littleton local fauna suggests that adaptive radiation of placentals may have begun within the first 400 Kyr of the Paleocene at least in the Denver Basin (Eberle 2003; Middleton and Dewar 2004). Other approaches to inferring ecology, such as dental complexity (Wilson and Self 2011), dental microwear (Calede and Wilson 2011; Christensen 2011), and postcranial data (Borths and Hunter 2008; Berg 2011), will also improve our understanding of this critical interval in mammalian evolution.

Acknowledgments

I would like to thank W. A. Clemens, H. J. Garbani, J. D. Archibald, D. L. Lofgren, G. Bennett, and all of their field and lab crews and mine that have recovered the fossils available for this study. For instruction, guidance, and custom software development for geometric morphometric analyses, I would especially like to thank M. Zelditch, H. D. Sheets, and D. Swiderski. For discussions on geometric morphometrics and dental functional morphology, I am also grateful to A. Aronowsky, K. Angielczyk, A. Evans, J. Jernvall, W. A. Clemens, J. Case, and P. Holroyd. D. Vilhena provided help with the analysis of body-size selectivity. I also express my gratitude to C. Strömberg, J. A. Wilson, M. Chen, L. Berg, D.

DeMar, J. Caledo, Z.-X. Luo, and two anonymous reviewers for their constructive suggestions to improve this manuscript.

Literature Cited

- Alroy, J. 1999. The fossil record of North American mammals: evidence for a Paleocene evolutionary radiation. *Systematic Biology* 48:107–118.
- . 2000. New methods for quantifying macroevolutionary patterns and processes. *Paleobiology* 26:707–733.
- Alvarez, W. 1986. Toward a theory of impact crises. *Eos* 67:649, 653–655, 658.
- Anderson, T. W. 1958. An introduction to multivariate analysis. Wiley, New York.
- Archer, M. 1978. The nature of the molar-premolar boundary in marsupials and reinterpretation of the homology of marsupial cheekteeth. *Memoirs of the Queensland Museum* 18:157–164.
- Archibald, J. D. 1982. A study of Mammalia and geology across the Cretaceous-Tertiary boundary in Garfield County, Montana. University of California Publications in Geological Sciences 122:1–286.
- . 1983. Structure of the K-T mammal radiation in North America: speculations on turnover rates and trophic structure. *Acta Palaeontologica Polonica* 28:7–17.
- . 1993. The importance of phylogenetic analysis for the assessment of species turnover: a case history of Paleocene mammals in North America. *Paleobiology* 19:1–27.
- . 1996. Dinosaur extinction and the end of an era: what the fossils say. Columbia University Press, New York.
- . 2011. Extinction and radiation: how the fall of dinosaurs led to the rise of mammals. Johns Hopkins University Press, Baltimore.
- Archibald, J. D., and L. J. Bryant. 1990. Differential Cretaceous/Tertiary extinctions of nonmarine vertebrates: evidence from northeastern Montana. In V. L. Sharpton, and P. D. Ward, eds. *Global catastrophes in earth history: an interdisciplinary conference on impacts, volcanism, and mass mortality*. Geological Society of America Special Paper 247:549–562.
- Archibald, J. D., Y. Zhang, T. Harper, and R. L. Cifelli. 2011. *Protungulatum*, confirmed Cretaceous occurrence of an otherwise eutherian (placental?) mammal. *Journal of Mammalian Evolution* 18:153–161.
- Badgley, C. 2003. The multiple scales of biodiversity. *Paleobiology* 29:11–13.
- Bambach, R. K. 1977. Species richness in marine benthic habitats through the Phanerozoic. *Paleobiology* 3:152–167.
- Bapst, D. W., P. C. Bullock, M. J. Melchin, H. D. Sheets, and C. E. Mitchell. 2012. Graptoloid diversity and disparity became decoupled during the Ordovician mass extinction. *Proceedings of the National Academy of Sciences USA* 109:3428–3433.
- Behrensmeyer, A. K., R. W. Hook, C. Badgley, J. A. Boy, R. E. Chapman, P. Dodson, R. A. Gastaldo, R. W. Graham, L. D. Martin, P. E. Olsen, R. A. Spicer, R. E. Taggart, and M. V. H. Wilson. 1992. Paleoenvironmental contexts and taphonomic modes. Pp. 15–136 in A. K. Behrensmeyer, J. D. Damuth, W. A. DiMichele, R. Potts, H.-D. Sues, and S. L. Wing, eds. *Terrestrial ecosystems through time: evolutionary paleoecology of terrestrial plants and animals*. University of Chicago Press, Chicago.
- Benton, M. J. 1983. Dinosaur success in the Triassic: a non-competitive ecological model. *Quarterly Review of Biology* 58:29–55.
- . 1987. Progress and competition in macroevolution. *Biological Reviews* 62:305–338.
- . 1991. Extinction, biotic replacements, and clade interactions. Pp. 89–102 in E. C. Dudley, ed. *The unity of evolutionary biology*. Dioscorides Press, Portland, Ore.
- . 1995. Diversification and extinction in the history of life. *Science* 268:52–58.
- Berg, L. 2011. Mammalian femora from the Cretaceous-Paleogene boundary of northeastern Montana. *Journal of Vertebrate Paleontology* 31(Suppl. to 3):70A.
- Bininda-Emonds, O. R. P., M. Cardillo, K. E. Jones, R. D. E. MacPhee, R. M. D. Beck, R. Grenyer, S. A. Price, R. A. Vos, J. L. Gittleman, and A. Purvis. 2007. The delayed rise of present-day mammals. *Nature* 446:507–512.
- Bloch, J. I., K. D. Rose, and P. D. Gingerich. 1998. New species of *Batodonoides* (Lipotyphla, Geolabididae) from the Early Eocene of Wyoming: smallest known mammal? *Journal of Mammalogy* 79:804–827.
- Borths, M., and J. P. Hunter. 2008. Gimme shelter? Locomotor trends and mammalian survivorship at the K-Pg boundary. *Journal of Vertebrate Paleontology* 28:54–55A.
- Breithaupt, B. H. 1982. Paleontology and paleoecology of the Lance Formation (Maastrichtian), east flank of Rock Springs Uplift, Sweetwater County, Wyoming. *Contributions to Geology, University of Wyoming* 21:123–151.
- Bruce, P. 2012. Resampling stats Excel add-in, Version 4.0. Institute of Statistics Education, Arlington, Va.
- Brusatte, S. L., R. J. Butler, A. Prieto-Márquez, and M. A. Norell. 2012. Dinosaur morphological diversity and the end-Cretaceous extinction. *Nature Communications* 3:804–808.
- Buffetaut, E. 1984. Palaeontology: selective extinctions and terminal Cretaceous events. *Nature* 310:276.
- . 1990. Vertebrate extinctions and survival across the Cretaceous-Tertiary boundary. *Tectonophysics* 171:337–345.
- Caledo, J. J., and G. P. Wilson. 2011. The last supper before the impact: mammalian diets across the Cretaceous-Paleogene boundary. *Journal of Vertebrate Paleontology* 31(Suppl. to No. 3):82A.
- Campione, N. E., and D. C. Evans. 2011. Cranial growth and variation in edmontosaurs (Dinosauria: Hadrosauridae): implications for latest Cretaceous megaherbivore diversity in North America. *PLoS ONE* 6:e25186.
- Case, J. A., F. J. Goin, and M. O. Woodburne. 2005. “South American” marsupials from the Late Cretaceous of North America and the origin of marsupial cohorts. *Journal of Mammalian Evolution* 12:461–494.
- Chenet, A.-L., V. Courtillot, F. Fluteau, M. Gerard, X. Quidelleur, S. Khadri, K. Sabbarao, and T. Thordarson. 2009. Determination of rapid Deccan eruptions across the Cretaceous-Tertiary boundary using paleomagnetic secular variation: constraints from analysis of eight new sections and synthesis for a 3500-m-thick composite section. *Journal of Geophysical Research* 114:1–38.
- Christensen, H. 2011. Mammalian community change after the K/T extinction in North America. *Geological Society of America Abstracts with Programs* 43:543.
- Ciampaglio, C. N. 2002. Determining the role that ecological and developmental constraints play in controlling disparity: examples from the crinoid and blastozoan fossil record. *Evolution and Development* 4:170–188.
- . 2004. Measuring changes in articulate brachiopod morphology before and after the Permian mass extinction event: do developmental constraints limit morphological innovation. *Evolution and Development* 6:260–274.
- Ciampaglio, C. N., M. Kemp, and D. W. McShea. 2001. Detecting changes in morphospace occupation patterns in the fossil record: characterization and analysis of measures of disparity. *Paleobiology* 27:695–715.
- Cifelli, R. L., J. J. Eberle, D. L. Lofgren, J. A. Lillegraven, and W. A. Clemens. 2004. Mammalian biochronology of the latest Cretaceous. Pp. 21–42 in M. O. Woodburne, ed. *Late Cretaceous and*

- Cenozoic mammals of North America: biostratigraphy and geochronology. Columbia University Press, New York.
- Clemens, W. A. 1964. Fossil mammals of the type Lance Formation, Wyoming, Part I. Introduction and Multituberculata. University of California Publications in Geological Sciences 48:1–105.
- . 1966. Fossil mammals of the type Lance Formation, Wyoming, Part II. Marsupialia. University of California Publications in Geological Sciences 62:1–122.
- . 1968. A mandible of *Didelphodon vorax* (Marsupialia, Mammalia). Los Angeles County Museum Contributions in Science 133:1–11.
- . 1973. Fossil mammals of the type Lance Formation, Wyoming, Part III. Eutheria and summary. University of California Publications in Geological Sciences 94:1–102.
- . 2001. Patterns of mammalian evolution across the Cretaceous-Tertiary boundary. *Mitteilungen aus dem Museum für Naturkunde in Berlin* 77:175–191.
- . 2002. Evolution of the mammalian fauna across the Cretaceous-Tertiary boundary in northeastern Montana and other areas of the Western Interior. Pp. 217–245 in Hartman et al. 2002.
- . 2004. *Purgatorius* (Plesiadapiformes, Primates?, Mammalia), a Paleocene immigrant into northeastern Montana: stratigraphic occurrences and incisor proportions. *Bulletin of the Carnegie Museum of Natural History* 36:3–13.
- . 2006. Early Paleocene (Puercan) peradectid marsupials from northeastern Montana, North American Western Interior. *Palaeontographica, Abteilung A* 277:19–31.
- . 2010. Were immigrants a significant part of the earliest Paleocene mammalian fauna of the North American Western Interior? *Vertebrata Palasiatica* 48:285–307.
- . 2013. Cf. *Wortmania* from the early Paleocene of Montana and an evaluation of the fossil record of the initial diversification of the Taeniodonta (Mammalia). *Canadian Journal of Earth Sciences* 50:341–354.
- Clemens, W. A., and G. P. Wilson. 2009. Early Torrejonian mammalian local faunas from northeastern Montana, U.S.A. *Museum of Northern Arizona Bulletin* 65:111–158.
- Collinson, M. E., and J. J. Hooker. 1991. Fossil evidence of interactions between plants and plant-eating mammals. *Philosophical Transactions of the Royal Society of London B* 333:197–208.
- Damuth, J. 1990. Problems in estimating body masses of archaic ungulates using dental measurements. Pp. 229–253 in Damuth and MacFadden 1990.
- Damuth, J., and B. J. MacFadden, eds. 1990. *Body size in mammalian paleobiology: estimation and biological implications*. Cambridge University Press, Cambridge.
- Davis, B. M. 2007. A revision of “pediomyid” marsupials from the Late Cretaceous of North America. *Acta Palaeontologica Polonica* 52:217–256.
- Dayrat, B. 2005. Ancestor-descendant relationships and the reconstruction of the Tree of Life. *Paleobiology* 31:347–353.
- Donohue, S. L., G. P. Wilson, and B. H. Breithaupt. 2013. Latest Cretaceous multituberculates of the Black Butte Station local fauna (Lance Formation, southwestern Wyoming) with implications for compositional differences among mammalian local faunas of the Western Interior. *Journal of Vertebrate Paleontology* 33(3) (in press).
- Droser, M. L., D. J. Bottjer, and P. M. Sheehan. 1997. Evaluating the ecological architecture of major events in the Phanerozoic history of marine invertebrate life. *Geology* 25:167–170.
- Eberle, J. J. 2003. Puercan mammalian systematics and biostratigraphy in the Denver Formation, Denver Basin, Colorado. *Rocky Mountain Geology* 38:143–169.
- Erwin, D. H. 1992. A preliminary classification of evolutionary radiations. *Historical Biology* 6:133–147.
- . 1998. The end and the beginning: recoveries from mass extinctions. *Trends in Ecology and Evolution* 13:344–349.
- . 2001. Lessons from the past: biotic recoveries from mass extinctions. *Proceedings of the National Academy of Sciences USA* 98:5399–5403.
- . 2008. Extinction as the loss of evolutionary history. *Proceedings of the National Academy of Sciences USA* 105:11520–11527.
- Evans, A. R., G. P. Wilson, M. Fortelius, and J. Jernvall. 2007. High-level similarity of dentitions in carnivores and rodents. *Nature* 445:78–81.
- Fara, E. 2000. Diversity of Callovian-Ypresian (Middle Jurassic-Eocene) tetrapod families and selectivity of extinctions at the K/T boundary. *Geobios* 33:387–396.
- Foote, M. 1993a. Discordance and concordance between morphological and taxonomic diversity. *Paleobiology* 19:185–204.
- . 1993b. Contributions of individual taxa to overall morphological diversity. *Paleobiology* 19:403–419.
- . 1997. The evolution of morphological diversity. *Annual Review of Ecology and Systematics* 28:129–152.
- Foote, M., and S. J. Gould. 1992. Cambrian and Recent morphological disparity. *Science* 258:1816.
- Foote, M., J. P. Hunter, C. M. Janis, and J. J. Sepkoski Jr. 1999. Evolutionary and preservational constraints on origins of biologic groups: divergence times of eutherian mammals. *Science* 283:1310–1314.
- Fortelius, M. 1990. Problems with using fossil teeth to estimate body sizes of extinct mammals. Pp. 207–228 in Damuth and MacFadden 1990.
- Fox, R. C. 1971. Early Campanian multituberculates (Mammalia: Allotheria) from the upper Milk River Formation, Alberta. *Canadian Journal of Earth Sciences* 8:916–938.
- . 1987. Palaeontology and the early evolution of marsupials. Pp. 161–169 in M. Archer, ed. *Possums and opossums: studies in evolution*. Surrey Beatty and the Royal Zoological Society of New South Wales, Sydney.
- . 1989. The Wounded Knee local fauna and mammalian evolution near the Cretaceous-Tertiary boundary, Saskatchewan, Canada. *Palaeontographica, Abteilung A* 208:11–59.
- Fox, R. C., and B. G. Naylor. 2006. Stagodontid marsupials from the Late Cretaceous of Canada and their systematic and functional implications. *Acta Palaeontologica Polonica* 51:13–36.
- Fox, R. C., C. S. Scott, and H. N. Bryant. 2007. A new, unusual therian mammal from the Upper Cretaceous of Saskatchewan, Canada. *Cretaceous Research* 28:821–829.
- Friedman, M. 2010. Explosive morphological diversification of spiny-finned teleost fishes in the aftermath of the end-Cretaceous extinction. *Proceedings of the Royal Society of London B* 277:1675–1683.
- Gibbs, S., M. Collard, and B. Wood. 2000. Soft-tissue characters in higher primate phylogenetics. *Proceedings of the National Academy of Sciences USA* 97:11130–11132.
- Goldin, T. J., and H. J. Melosh. 2009. Self-shielding of thermal radiation by Chicxulub impact ejecta: firestorm or fizzle? *Geology* 37:1135–1138.
- Gordon, C. L. 2003. *Functional morphology and diet of Late Cretaceous mammals of North America*. Ph.D. dissertation. University of Oklahoma, Norman.
- Goswami, A. 2012. A dating success story: genomes and fossils converge on placental mammal origins. *EvoDevo* 3:18.
- Gould, S. J. 1985. The paradox of the first tier: an agenda for paleobiology. *Paleobiology* 11:2–12.
- . 1991. The disparity of the Burgess Shale arthropod fauna and the limits of cladistic analysis: why we must strive to quantify morphospace. *Paleobiology* 17:411–423.

- . 2002. The structure of evolutionary theory. Belknap Press of Harvard University Press, Cambridge.
- Hartman, J. H., K. R. Johnson, and D. J. Nichols, eds. 2002. The Hell Creek Formation and the Cretaceous-Tertiary boundary in the northern Great Plains: an integrated continental record of the end of the Cretaceous. Geological Society of America Special Paper 361.
- Horovitz, I., T. Martin, J. Bloch, S. Ladevèze, C. Kurz, and M. Sánchez-Villagra. 2009. Cranial anatomy of the earliest marsupials and the origin of opossums. *PLoS ONE* 4:1–9.
- Hotton, C. L. 2002. Palynology of the Cretaceous-Tertiary boundary in central Montana: evidence for extraterrestrial impact as a cause of the terminal Cretaceous extinctions. Pp. 473–501 in Hartman et al. 2002.
- Hunter, J. P. 1997. Adaptive radiation of Early Paleocene ungulates. Ph.D. dissertation. State University of New York, Stony Brook.
- Hunter, J. P., and J. D. Archibald. 2002. Mammals from the end of the age of dinosaurs in North Dakota and southeastern Montana, with a reappraisal of geographic differentiation among Lancian mammals. Pp. 191–216 in Hartman et al. 2002.
- Hunter, J. P., and J. Jernvall. 1995. The hypocone as a key innovation in mammalian evolution. *Proceedings of the National Academy of Sciences USA* 92:10718–10722.
- Hunter, J. P., J. H. Hartman, and D. W. Krause. 1997. Mammals and mollusks across the Cretaceous-Tertiary boundary from Makoshika State Park and vicinity (Williston Basin), Montana: University of Wyoming Contributions to Geology 32:61–114.
- Jablonski, D. 1986. Background and mass extinctions: the alternation of macroevolutionary regimes. *Science* 231:129–133.
- . 1998. Geographic variation in the molluscan recovery from the end-Cretaceous extinction. *Science* 279:1327–1330.
- . 2005. Mass extinctions and macroevolution. In E. S. Vrba and N. Eldredge, eds. *Macroevolution: diversity, disparity, contingency*. *Paleobiology* 31(Suppl. to No. 2):192–210.
- Jablonski, D., and D. Raup. 1995. Selectivity of end-Cretaceous marine bivalve extinctions. *Science* 268:389–391.
- Jablonski, D., K. Roy, J. W. Valentine, R. M. Price, and P. S. Anderson. 2003. The impact of the pull of the Recent on the history of marine diversity. *Science* 300:1133–1135.
- Janis, C. M. 1990. Correlation of cranial and dental variables with body size in ungulates and macropodoids. Pp. 255–300 in Damuth and MacFadden 1990.
- Janzen, D. H. 1995. Who survived the Cretaceous? *Science* 268:785.
- Jernvall, J. 2000. Linking development with generation of novelty in mammalian teeth. *Proceedings of the National Academy of Sciences USA* 97:2641–2645.
- Jernvall, J., J. P. Hunter, and M. Fortelius. 2000. Trends in the evolution of molar crown types in ungulate mammals: evidence from the Northern Hemisphere. Pp. 269–281 in M. F. Teaford, M. M. Smith, and M. W. J. Ferguson, eds. *Development, function, and evolution of teeth*. Cambridge University Press, New York.
- Johanson, Z. 1996. Revision of the Late Cretaceous North American marsupial genus *Alphadon*. *Palaeontographica, Abteilung A* 242:127–184.
- Kangas, A. T., A. R. Evans, I. Thesleff, and J. Jernvall. 2004. Nonindependence of mammalian dental characters. *Nature* 432:211–214.
- Kay, R. F. 1975. The functional adaptations of primate molar teeth. *American Journal of Physical Anthropology* 43:195–216.
- Kendall, D. 1977. The diffusion of shape. *Advances in Applied Probability* 9:428–430.
- Kielan-Jaworowska, Z., R. L. Cifelli, and Z.-X. Luo. 2004. Mammals from the Age of Dinosaurs: origins, evolution, and structure. Columbia University Press, New York.
- Kiessling, W., and R. C. Baron-Szabo. 2004. Extinction and recovery patterns of scleractinian corals at the Cretaceous-Tertiary boundary. *Palaeogeography, Palaeoclimatology, Palaeoecology* 214:195–223.
- Krause, D. W. 1982. Jaw movement, dental function, and diet in the Paleocene multituberculate *Ptilodus*. *Paleobiology* 8:265–281.
- Krug, A. Z., and D. Jablonski. 2012. Long-term origination rates are reset only at mass extinctions. *Geology* 40:731–734.
- Krug, A. Z., D. Jablonski, and J. W. Valentine. 2009. Signature of the end-Cretaceous mass extinction in the modern biota. *Science* 323:767–771.
- Levine, J. M., and C. M. D'Antonio. 1999. Elton revisited: a review of evidence linking diversity and invasibility. *Oikos* 87:15–26.
- Levinton, J. S. 1996. Trophic group and the end-Cretaceous extinction: did deposit feeders have it made in the shade? *Paleobiology* 22:104–112.
- Lillegraven, J. A. 1969. Latest Cretaceous mammals of upper part of Edmonton Formation of Alberta, Canada, and review of marsupial-placental dichotomy in mammalian evolution. *University of Kansas Paleontological Contributions* 50:1–122.
- . 1972. Ordinal and familial diversity of Cenozoic mammals. *Taxon* 21:261–274.
- Lillegraven, J. A., and J. J. Eberle. 1999. Vertebrate faunal changes through Lancian and Puercan time in southern Wyoming. *Journal of Paleontology* 73:691–710.
- Lockwood, R. 2004. The K/T event and infaunality: morphological and ecological patterns of extinction and recovery in veneroid bivalves. *Paleobiology* 30:507–521.
- . 2005. Body size, extinction events, and the early Cenozoic record of veneroid bivalves: a new role for recoveries? *Paleobiology* 31:578–590.
- Lofgren, D. L. 1992. Upper premolar configuration of *Didelphodon vorax* (Mammalia, Marsupialia, Stagodontidae). *Journal of Paleontology* 66:162–164.
- . 1995. The Bug Creek Problem and the Cretaceous-Tertiary transition at McGuire Creek, Montana. *University of California Publications in Geological Sciences* 140:1–185.
- Lofgren, D. L., C. L. Hotton, and A. C. Runkel. 1990. Reworking of Cretaceous dinosaurs into Paleocene channel deposits, upper Hell Creek Formation, Montana. *Geology* 18:874–877.
- Lofgren, D. L., J. A. Lillegraven, W. A. Clemens, P. D. Gingerich, and T. E. Williamson. 2004. Paleocene biochronology: the Puercan through Clarkforkian land mammal ages. Pp. 43–105 in M. O. Woodburne, ed. *Late Cretaceous and Cenozoic mammals of North America: biostratigraphy and geochronology*. Columbia University Press, New York.
- Lucas, P. W. 2004. *Dental functional morphology: how teeth work*. Cambridge University Press, Cambridge.
- Luckett, W. P. 1993. An ontogenetic assessment of dental homologies in therian mammals. Pp. 182–204 in F. S. Szalay, M. J. Novacek, and M. C. McKenna, eds. *Mammal phylogeny: Mesozoic differentiation, multituberculates, monotremes, early therians, and marsupials*. Springer, New York.
- Luo, Z.-X. 2007. Transformation and diversification in early mammalian evolution. *Nature* 450:1011–1019.
- Lupia, R. 1999. Discordant morphological disparity and taxonomic diversity during the Cretaceous angiosperm radiation: North American pollen record. *Paleobiology* 25:1–28.
- Maas, M. C., and D. W. Krause. 1994. Mammalian turnover and community structure in the Paleocene of North America. *Historical Biology* 8:91–128.
- Maas, M. C., M. R. L. Anthony, P. D. Gingerich, G. F. Gunnell, and D. W. Krause. 1995. Mammalian generic diversity and turnover in the Late Paleocene and Early Eocene of the Bighorn and Crazy Mountains Basins, Wyoming and Montana. *Palaeogeography, Palaeoclimatology, Palaeoecology* 115:181–207.
- MacLeod, N., and G. Keller, eds. 1996. *Cretaceous-Tertiary mass extinctions: biotic and environmental changes*. W. W. Norton, New York.

- Markwick, P. J. 1998. Crocodylian diversity in space and time: the role of climate in paleoecology and its implication for understanding K/T extinctions. *Paleobiology* 24:470–497.
- Marshall, C. R., and P. D. Ward. 1996. Sudden and gradual molluscan extinctions in the latest Cretaceous of Western European Tethys. *Science* 274:1360–1363.
- McGhee, G. R., Jr., P. M. Sheehan, D. J. Bottjer, and M. L. Droser. 2004. Ecological ranking of Phanerozoic biodiversity crises: ecological and taxonomic severities are decoupled. *Palaeogeography, Palaeoclimatology, Palaeoecology* 211:289–297.
- McGowan, A. J. 2004. Ammonoid taxonomic and morphological recovery patterns after the Permian-Triassic. *Geology* 32:665–668.
- McKenna, M. C. 1975. Toward a phylogenetic classification of the Mammalia. Pp. 21–46 in W. P. Luckett and F. S. Szalay, eds. *Phylogeny of the primates*. Plenum, New York.
- McKinney, M. L. 1997. Extinction vulnerability and selectivity: combining ecological and paleontological views. *Annual Review of Ecology and Systematics* 28:495–516.
- Meredith, R. W., J. E. Janečka, J. Gatesy, O. A. Ryder, C. A. Fisher, E. C. Teeling, A. Goodbla, E. Eizirik, T. L. Simão, T. Stadler, D. L. Rabosky, R. L. Honeycutt, J. J. Flynn, C. M. Ingram, C. Steiner, T. L. Williams, T. J. Robinson, A. Burk-Herrick, M. Westerman, N. A. Ayoub, M. S. Springer, and W. J. Murphy. 2011. Impacts of the Cretaceous terrestrial revolution and KPg extinction on mammal diversification. *Science* 334:521–524.
- Middleton, M. D., and E. W. Dewar. 2004. New mammals from the early Paleocene Littleton fauna (Denver Formation, Colorado). In S. G. Lucas, K. E. Zeigler, and P. E. Kondrashov, eds. *Paleogene mammals*. New Mexico Museum of Natural History and Science Bulletin 26:59–80.
- Montellano, M. 1992. Mammalian fauna of the Judith River Formation (Late Cretaceous, Judithian), northcentral Montana. University of California Publications in Geological Sciences 136:1–115.
- Moore, J. R., G. P. Wilson, M. Sharma, H. R. Hallock, and D. R. Braman. In press. Assessing the relationships of the Hell Creek–Fort Union contact, Cretaceous–Paleogene boundary and impact ejecta horizon at the type section of the Hell Creek Formation, Montana, U.S.A. In G. P. Wilson, W. A. Clemens, J. R. Horner, and J. H. Hartman, eds. *Through the end of the Cretaceous in the type locality of the Hell Creek Formation in Montana and adjacent areas*. Geological Society of America Special Paper.
- Murphy, W. J., D. M. Larkin, A. Everts-van der Wind, G. Bourque, G. Tesler, L. Auvil, J. E. Beever, B. P. Chowdhary, F. Galibert, L. Gatzke, C. Hitte, S. N. Meyers, D. Milan, E. A. Ostrander, G. Pape, H. G. Parker, T. Raudsepp, M. B. Rogatcheva, L. B. Schook, L. C. Skow, M. Welge, J. E. Womack, S. J. O'Brien, P. A. Pevzner, and H. A. Lewin. 2005. Dynamics of mammalian chromosome evolution inferred from multispecies comparative maps. *Science* 309:613–617.
- Naylor, G. J., and D. C. Adams. 2001. Are the fossil data really at odds with the molecular data? Morphological evidence for Cetartiodactyla phylogeny reexamined. *Systematic Biology* 50:444–453.
- Nichols, D. J., and K. R. Johnson. 2008. *Plants and the K-T Boundary*. Cambridge University Press, New York.
- Norris, R. D. 1991. Biased extinction and evolutionary trends. *Paleobiology* 17:388–399.
- Novacek, M., and W. A. Clemens. 1977. Aspects of intrageneric variation and evolution of *Mesodma* (Multituberculata, Mammalia). *Journal of Paleontology* 51:701–717.
- Ogg, J. G., and A. G. Smith. 2004. The geomagnetic polarity time scale. Pp. 63–86 in F. M. Gradstein, J. G. Ogg, and A. G. Smith, eds. *A geologic time scale 2004*. Cambridge University Press, Cambridge.
- Payne, J. L., and S. Finnegan. 2007. The effect of geographic range on extinction risk during background and mass extinction. *Proceedings of the National Academy of Sciences USA* 104:10506–10511.
- Raup, D. 1986. Biological extinction in earth history. *Science* 231:1528–1533.
- . 1991. *Extinction: bad genes or bad luck?* W. W. Norton, New York.
- Raup, D., and D. Jablonski. 1993. Geography of end-Cretaceous marine bivalve extinctions. *Science* 260:971–973.
- Renne, P. R., G. Balco, K. R. Ludwig, R. Mundil, and K. Min. 2011. Response to the comment by W. H. Schwartz et al. on “Joint determination of ^{40}K decay constants and $^{40}\text{Ar}^*/^{40}\text{K}$ for the Fish Canyon sanidine standard, and improved accuracy for the $^{40}\text{Ar}/^{39}\text{Ar}$ geochronology” by P. R. Renne et al. (2010). *Geochimica et Cosmochimica Acta* 75:5097–5100.
- Robertson, D. S., M. C. McKenna, O. B. Toon, S. Hope, and J. A. Lillegraven. 2004. Survival in the first hours of the Cenozoic. *Geological Society of America Bulletin* 116:760–768.
- Rohlf, F. J. 1990. Morphometrics. *Annual Review of Ecology and Systematics* 21:299–316.
- . 2010a. tpsDig, Version 2.16. Department of Ecology and Evolution, State University of New York, Stony Brook.
- . 2010b. tpsUtil, Version 1.46. Department of Ecology and Evolution, State University of New York, Stony Brook.
- Rosenzweig, M. L., and R. D. McCord. 1991. Incumbent replacement: evidence for long-term evolutionary progress. *Paleobiology* 17:202–213.
- Salazar-Ciudad, I., and J. Jernvall. 2002. A gene network model accounting for development and evolution of mammalian teeth. *Proceedings of the National Academy of Sciences USA* 99:8116–8120.
- Schulte, P., L. Alegret, I. Arenillas, J. A. Arz, P. J. Barton, P. R. Bown, T. J. Bralower, G. L. Christeson, P. Claeys, C. S. Cockell, G. S. Collins, A. Deutsch, T. J. Goldin, K. Goto, J. M. Grajales-Nishimura, R. A. F. Grieve, S. P. S. Gulick, K. R. Johnson, W. Kiessling, C. Koeberl, D. A. Kring, K. G. MacLeod, T. Matsui, J. Melosh, A. Montanari, J. V. Morgan, C. R. Neal, D. J. Nichols, R. D. Norris, E. Pierazzo, G. Ravizza, M. Rebolledo-Vieyra, W. U. Reimold, E. Robin, T. Salge, R. P. Speijer, A. R. Sweet, J. Urrutia-Fucugauchi, V. Vajda, M. T. Whalen, and P. S. Willumsen. 2010. The Chicxulub asteroid impact and mass extinction at the Cretaceous–Paleogene boundary. *Science* 327:1214–1218.
- Sheehan, P. M., and D. E. Fastovsky. 1992. Major extinctions of land-dwelling vertebrates at the Cretaceous–Tertiary boundary, eastern Montana. *Geology* 20:556–560.
- Sheehan, P. M., and T. A. Hansen. 1986. Detritus feeding as a buffer to extinction at the end of the Cretaceous. *Geology* 14:868–870.
- Sheehan, P. M., P. J. Coorough, and D. Fastovsky. 1996. Biotic selectivity during the K/T and Late Ordovician extinction events. In G. Ryder, D. Fastovsky, and S. Gartner, eds. *The Cretaceous–Tertiary event and other catastrophes in earth history*. Geological Society of America Special Paper 307:477–489.
- Sheets, H. D. 2003. CoordGen for integrated morphometrics package, Version 6f. Department of Physics, Canisius College, Buffalo, N.Y.
- . 2007. DisparityBox for integrated morphometrics package, Version 6i. Department of Physics, Canisius College, Buffalo, N.Y.
- . 2009. Semiland for integrated morphometrics package, Version 6. Department of Physics, Canisius College, Buffalo, N.Y.
- . 2012. PCAGenMac for integrated morphometrics package, Version 7a. Department of Physics, Canisius College, Buffalo, N.Y.

- Simpson, G. G. 1937. The beginning of the Age of Mammals. *Biological Reviews* 12:1–47.
- . 1952. Periodicity in vertebrate evolution. *Journal of Paleontology* 26:359–370.
- Sloan, R. E. 1979. Multituberculata. Pp. 492–498 in R. W. Fairbridge and D. Jablonski, eds. *The Encyclopedia of Paleontology*. Dowden, Hutchinson and Ross, Stroudsburg, Pa.
- Sloan, R. E., and L. Van Valen. 1965. Cretaceous mammals from Montana. *Science* 148:220–227.
- Smith, A. B., and C. H. Jeffery. 1998. Selectivity of extinction among sea urchins at the end of the Cretaceous period. *Nature* 392:69–71.
- Smith, F. A., A. G. Boyer, J. H. Brown, D. P. Costa, T. Dayan, S. K. M. Ernest, A. R. Evans, M. Fortelius, J. L. Gittleman, M. J. Hamilton, L. E. Harding, K. Lintulaakso, S. K. Lyons, C. McCain, J. G. Okie, J. J. Saarinen, R. M. Sibly, P. R. Stephens, J. Theodor, and M. D. Uhen. 2010. The evolution of maximum body size of terrestrial mammals. *Science* 330:1216–1219.
- Smits, P., and G. P. Wilson. 2011. Estimates and trends in body size of Laurasian Cretaceous mammals. In K. Trinajstić, M. Bunce, N. Warburton, C. Hadley, A. Baynes, and M. Siverson, eds. *Thirteenth Conference on Australasian Vertebrate Evolution Paleontology and Systematics*. Geological Survey of Western Australia, Record 2011/9:76. Perth.
- Solé, R. V., J. M. Montoya, and D. H. Erwin. 2002. Recovery after mass extinction: evolutionary assembly in large-scale biosphere dynamics. *Philosophical Transactions of the Royal Society of London B* 357:697–707.
- Storer, J. E. 1991. The mammals of the Gryde Local Fauna, Frenchman Formation (Maastrichtian: Lancian), Saskatchewan. *Journal of Vertebrate Paleontology* 11:350–369.
- Strait, S. G. 1993. Molar morphology and food texture among small-bodied insectivorous mammals. *Journal of Mammalogy* 72:391–402.
- . 1997. Tooth use and the physical properties of food. *Evolutionary Anthropology* 5:199–211.
- Stucky, R. K. 1990. Evolution of land mammal diversity in North America during the Cenozoic. Pp. 375–432 in H. H. Genoways, ed. *Current mammalogy*, Vol. 2. Plenum, New York.
- Swisher, C. C., III, L. Dingus, and R. F. Butler. 1993. $^{40}\text{Ar}/^{39}\text{Ar}$ dating and magnetostratigraphic correlation of the terrestrial Cretaceous-Paleogene boundary and Puercan Mammal Age, Hell Creek-Tullock formations, eastern Montana. *Canadian Journal of Earth Sciences* 30:1981–1986.
- Tedford, R. H. 1970. Principles and practices of mammalian geochronology in North America. Pp. 666–703 in E. L. Yochelson, ed. *Proceedings of the North American Paleontological Convention*. Allen Press, Lawrence, Kans.
- Tseng, Z. J., and X. Wang. 2011. Do convergent ecomorphs evolve through convergent morphological pathways? Cranial shape evolution in fossil hyaenids and borophagine canids (Carnivora, Mammalia). *Paleobiology* 37:470–489.
- Van Valen, L. M. 1971. Adaptive zones and the orders of mammals. *Evolution* 25:420–428.
- . 1978. The beginning of the Age of Mammals. *Evolutionary Theory* 4:45–80.
- Van Valen, L. M., and R. E. Sloan. 1977. Ecology and the extinction of the dinosaurs. *Evolutionary Theory* 2:37–64.
- Vilhena, D. A., E. B. Harris, C. T. Bergstrom, M. E. Maliska, C. A. Sidor, P. Ward, C. A. E. Strömberg, and G. P. Wilson. 2012. A molluscan latitudinal selectivity gradient in the end-Cretaceous mass extinction. *Geological Society of America Abstracts with Programs* 44:185.
- Villier, L., and D. Korn. 2004. Morphological disparity of ammonoids and the mark of Permian mass extinctions. *Science* 306:264–266.
- Wagner, P. J. 1995. Testing evolutionary constraint hypotheses with early Paleozoic gastropods. *Paleobiology* 21:248–272.
- Weil, A. 1998. A new species of *Microcosmodon* (Mammalia: Multituberculata) from the Paleocene Tullock Formation of Montana, and an argument for the Microcosmodontidae. *PaleoBios* 18:1–15.
- . 1999. Multituberculate phylogeny and mammalian biogeography in the Late Cretaceous and earliest Paleocene Western Interior of North America. Ph.D. dissertation. University of California, Berkeley.
- Weil, A., and W. A. Clemens. 1998. Aliens in Montana: phylogenetically and biogeographically diverse lineages contributed to an earliest Cenozoic community. *Geological Society of America Abstracts with Programs* 30:69–70.
- Wesley-Hunt, G. D. 2005. The morphological diversification of carnivores in North America. *Paleobiology* 31:35–55.
- Wilf, P., C. C. Labandeira, K. R. Johnson, and B. Ellis. 2006. Decoupled plant and insect diversity after the end-Cretaceous Extinction. *Science* 313:1112–1115.
- Williamson, T. E., S. L. Brusatte, T. D. Carr, A. Weil, and B. R. Standhardt. 2012. The phylogeny and evolution of Cretaceous-Paleogene metatherians: cladistic analysis and description of new early Paleocene specimens from the Nacimiento Formation, New Mexico. *Journal of Systematic Palaeontology* 10:625–651.
- Wilson, G. P. 2004. A quantitative assessment of mammalian change leading up to and across the Cretaceous-Tertiary boundary in northeastern Montana. Ph.D. dissertation. University of California, Berkeley.
- . 2005. Mammalian faunal dynamics during the last 1.8 million years of the Cretaceous in Garfield County, Montana. *Journal of Mammalian Evolution* 12:53–75.
- . In press. Mammalian extinction, survival, and recovery dynamics across the Cretaceous-Paleogene boundary in northeastern Montana. In G. P. Wilson, W. A. Clemens, J. R. Horner, and J. H. Hartman, eds. *Through the end of the Cretaceous in the type locality of the Hell Creek Formation in Montana and adjacent areas*. Geological Society of America Special Papers.
- Wilson, G. P., and J. A. Riedel. 2010. New specimen reveals deltatheroidan affinities of the North American Late Cretaceous mammal *Nanocuris*. *Journal of Vertebrate Paleontology* 30:872–884.
- Wilson, G. P., and C. Self. 2011. Mammalian dental complexity across the Cretaceous-Paleogene boundary with implications for ecological recovery and expansion. *Journal of Vertebrate Paleontology* 31(Suppl. to No. 3):215A.
- Wilson, G. P., M. Dechesne, and I. R. Anderson. 2010. New latest Cretaceous mammals from northeastern Colorado with biochronologic and biogeographic implications. *Journal of Vertebrate Paleontology* 30:499–520.
- Wilson, G. P., A. R. Evans, I. J. Corfe, P. D. Smits, M. Fortelius, and J. Jernvall. 2012. Adaptive radiation of multituberculate mammals before the extinction of dinosaurs. *Nature* 483:457–460.
- Wing, S. L., and B. H. Tiffney. 1987. Interactions of angiosperms and herbivorous tetrapods through time. Pp. 203–224 in E. M. Friis, W. G. Chaloner, and P. R. Crane, eds. *The origins of angiosperms and their biological consequences*. Cambridge University Press, New York.
- Wing, S. L., H.-D. Sues, R. Potts, W. A. DiMichele, and A. K. Behrensmeyer. 1992. Evolutionary paleoecology. Pp. 1–13 in A. K. Behrensmeyer, J. Damuth, W. A. DiMichele, R. Potts, H.-D. Sues, and S. L. Wing, eds. *Terrestrial ecosystems through time: evolutionary paleoecology of terrestrial plants and animals*. University of Chicago Press, Chicago.
- Zelditch, M. L., D. L. Swiderski, H. D. Sheets, and W. L. Fink. 2004. *Geometric morphometrics for biologists: a primer*. Elsevier Academic, San Diego.